

Covariance Estimation for Matrix-valued Data

Yichi Zhang

Department of Statistics, North Carolina State University

Weining Shen

Department of Statistics, University of California, Irvine

Dehan Kong

Department of Statistical Sciences, University of Toronto

April 14, 2020

Abstract

Covariance estimation for matrix-valued data has received an increasing interest in applications including neuroscience and environmental studies. Unlike previous works that rely heavily on matrix normal distribution assumption and the requirement of fixed matrix size, we propose a class of distribution-free regularized covariance estimation methods for high-dimensional matrix data under a separability condition and a bandable covariance structure. Under these conditions, the original covariance matrix is decomposed into a Kronecker product of two bandable small covariance matrices representing the variability over row and column directions. We formulate a unified framework for estimating the banded and tapering covariance, and introduce an efficient algorithm based on rank one unconstrained Kronecker product approximation. The convergence rates of the proposed estimators are studied and compared to the ones for the usual vector-valued data. We further introduce a class of robust covariance estimators and provide theoretical guarantees to deal with the potential heavy-tailed data. We demonstrate the superior finite-sample performance of our methods using simulations and real applications from an electroencephalography study and a gridded temperature anomalies dataset.

Keywords: Bandable; Distribution-free, Neuroimaging; Robust; Separable.

1 Introduction

Matrix-valued data have received considerable interests in various applications. For example, in brain imaging studies, multi-channel electroencephalography (EEG) is often employed to determine the locations and time courses of the underlying electric current sources. These sources can be elicited by a stimulus or several stimuli in electrical, auditory and visual channels. The collected EEG data can often be represented as a matrix with a spatial dimension to record the electric locations and a temporal dimension for repeated measurements over a continuous range of time. Another common example is in environmental studies, where the outcome of interest (e.g., temperature, humidity, air quality) is measured over a range of geographical regions. It is hence natural to represent the resulting data in a matrix form with two dimensions corresponding to latitude and longitude. Examples of matrix-valued data also include two-dimensional digital imaging data, brain surface data and colorimetric sensor array data. There have been a few recent studies on regression analysis for matrix-valued data (Zhou and Li, 2014; Wang and Zhu, 2017; Kong et al., 2020).

In this paper, we are interested in estimating the covariance of the matrix-valued data. Covariance estimation is a fundamental problem in multivariate data analysis. A large collection of statistical and machine learning methodologies including the principal component analysis, linear discriminant analysis, regression analysis and clustering analysis, require the knowledge of the covariance matrices. Denote $\mathbf{X} \in \mathbb{R}^{p \times q}$ two dimensional matrix-valued data, and $\text{vec}(\cdot)$ the vectorization operator that stacks the columns of a matrix into a column vector. The covariance of \mathbf{X} is defined as $\text{cov}(\text{vec}(\mathbf{X})) = \Sigma^* \in \mathbb{R}^{pq \times pq}$. A naive estimate of Σ^* is the sample covariance. However, when $pq > n$, it performs poorly. It has been shown in Wachter et al. (1978); Johnstone (2001); Johnstone and Lu (2009) that when $pq/n \rightarrow c \in (0, \infty]$, the largest eigenvalue of the population covariance matrix is an inconsistent estimator of the largest eigenvalue for the sample covariance matrix, and the eigenvectors of the sample covariance matrix can be nearly orthogonal to the truth.

To overcome the ultra-high dimensionality, structural assumptions are needed to

estimate the covariance consistently. Various types of structured covariance matrices have been introduced such as bandable covariance matrices, sparse covariance matrices, spiked covariance matrices. Several regularization methods have been developed accordingly to estimate these matrices, including banded methods (Bickel and Levina, 2008b; Wu and Pourahmadi, 2009), tapering methods (Furrer and Bengtsson, 2007; Cai et al., 2010), and thresholding methods (Bickel and Levina, 2008a; El Karoui, 2008; Cai and Liu, 2011). Another issue with the sample covariance is that it does not utilize the knowledge that the data actually lie in a two dimensional matrix space. To address this issue, it is common to impose a separability assumption on the covariance of $\text{vec}(\mathbf{X})$, i.e. $\text{Cov}[\text{vec}(\mathbf{X})] = \mathbf{\Sigma}_2^* \otimes \mathbf{\Sigma}_1^*$, where $\mathbf{\Sigma}_1^* \in \mathbb{R}^{p \times p}$ and $\mathbf{\Sigma}_2^* \in \mathbb{R}^{q \times q}$ represent covariances among the rows and columns of the matrices, respectively. The separability assumption helps provide a stable and parsimonious alternative to an unrestricted version of $\text{Cov}[\text{vec}(\mathbf{X})]$, and equally importantly, renders for a simple-yet-meaningful scientific interpretation. For example, in MEG/EEG data analysis, the separability assumption allows us to project the variation within the imaging data onto spatial and temporal domains (De Munck et al., 2002). When analyzing temperature measurements over a geographical region, this assumption helps decompose the variability in the measurements onto spatial directions (e.g., longitude and latitude).

To account for the separability assumption when estimating the covariance of matrix-valued data, a class of methods were proposed in the literature, all based on assuming a matrix normal distribution for the data. This idea was first proposed by Dawid (1981), and then explored by Dutilleul (1999) as they introduced an iterative algorithm for maximum likelihood estimation. Werner, Jansson, and Stoica (2008) developed two alternative estimation methods and derived the Cramér-Lower bound for the problem in a compact form. Lu and Zimmerman (2005) and Mitchell, Genton, and Gumpertz (2006) developed likelihood ratio tests for separability of the covariance matrices. Beyond the matrix case, Galecki (1994) and Hoff (2011) considered separable covariance matrices estimation for tensor data under the tensor normal model. To summarize, all the aforementioned methods rely heavily on the

matrix normal distribution assumption since their estimation and testing procedures are obtained using maximum likelihood estimation (MLE). Moreover, these methods can only handle the matrices with fixed dimensions, especially for the development of asymptotic theory. It remains unclear how those methodologies can be generalized under realistic situations where the data do not satisfy a matrix normal distribution (or any presumed distribution) and how the asymptotic theory works for matrices with high dimensions.

In this paper, we consider the covariance estimation problem for matrix-valued data under a much more challenging but realistic scenario. First, our method is distribution-free, which significantly differs from all the previous likelihood approaches. Second, we allow the dimensions of the matrix-valued data to be much larger than the sample size, i.e. they can diverge at the exponential rate of the sample size. Under this scenario, even if the matrix normal assumption is true, the MLE still does not exist due to overfitting. Our solution is to impose a bandable assumption on Σ_1^* and Σ_2^* . This assumption has been widely adopted for time series with many scientific applications (Friston et al., 1994; Visser and Molenaar, 1995). The resulting bandable covariance structure exhibits a natural order among variables, thus can naturally depict the spatial and/or temporal correlation of the matrix-valued data. We then incorporate the separable and bandable properties into one unified estimation framework, and propose an efficient computational algorithm to obtain banded and tapering covariance estimates. The convergence rates of the proposed estimators are derived under the high dimensional setting; and then compared to the theoretical results obtained in Bickel and Levina (2008b) and Cai et al. (2010) for vector-valued data. The proof is based on matrix perturbation theory and sheds new insights on high-dimensional regularized covariance estimation when taking the matrix structure of the data into account. To deal with potentially heavy-tailed matrix-valued data, we have further proposed robust banded and tapering covariance estimators and provided theoretical support for the robust estimates. Both simulation studies and two data applications from an electroencephalography study and an analysis of a gridded temperature anomalies dataset have confirmed the excellent performance

of the proposed approaches.

The rest of the article is organized as follows. We introduce our banded and tapering covariance estimates of matrix-valued data in Section 2. Section 3 provides theoretical support of our proposed procedure. In Section 4, we further propose a robust banded and tapering covariance estimation procedure to deal with heavy-tailed data and provide theoretical guarantees. Simulations are conducted in Section 5 to evaluate the finite-sample performance of the proposed methods. In Section 6, we apply our method to an electroencephalography study and a gridded temperature anomalies dataset. We end with some discussions in Section 7. Technical proofs and additional numerical results are presented in the Supplementary File.

Notation: We summarize the notation used throughout the paper here. For a vector $\mathbf{w} \in \mathbb{R}^d$, we denote $\|\mathbf{w}\|$ its Euclidean norm. For a matrix $\mathbf{A} = [A_{ij}] \in \mathbb{R}^{d_1 \times d_2}$, we denote $\text{tr}(\mathbf{A})$ its trace and $\|\mathbf{A}\|_F$ its Frobenius norm. We also define the following matrix norms,

$$\begin{aligned}
\|\mathbf{A}\|_2 &\equiv \sup\{\|\mathbf{A}x\|_2, \|x\|_2 = 1\}, \\
\|\mathbf{A}\|_1 &\equiv \sup\{\|\mathbf{A}x\|_1, \|x\|_1 = 1\} = \max_j \sum_i |A_{ij}|, \\
\|\mathbf{A}\|_\infty &\equiv \sup\{\|\mathbf{A}x\|_{\max}, \|x\|_{\max} = 1\} = \max_i \sum_j |A_{ij}|, \\
\|\mathbf{A}\|_{\max} &\equiv \max_{i,j} |A_{ij}|, \|\mathbf{A}\|_{1,1} = \sum_i \sum_j |A_{ij}|.
\end{aligned} \tag{1.1}$$

For two matrices $\mathbf{A} \in \mathbb{R}^{p_A \times q_A}$ and $\mathbf{B} \in \mathbb{R}^{p_B \times q_B}$, their Kronecker product $\mathbf{A} \otimes \mathbf{B}$ is a $p_A p_B \times q_A q_B$ matrix. Define \circ to be the Hadamard product of two matrices, i.e. element-wise product, and $\lfloor \cdot \rfloor$ to be the floor function.

2 Methodology

Denote $\mathbf{X} \in \mathbb{R}^{p \times q}$ a two-dimensional random matrix, and $\text{vec}(\cdot)$ a vectorization operator that stacks the columns of a matrix into a vector. Let $\Sigma^* \in \mathcal{S}_+^{pq \times pq}$ be the true covariance matrix of $\text{vec}(\mathbf{X}_i)$, where $\mathcal{S}_+^{d \times d}$ denotes the space of $d \times d$ positive definite matrices. Assume that $\{\mathbf{X}_i : 1 \leq i \leq n\}$ are independently and identically

distributed (i.i.d.) matrix-valued samples generated from \mathbf{X} . The main interest of the paper is to estimate Σ^* from the sampled data, where we allow $p > n$ and $q > n$.

A naive estimator of Σ^* is the sample covariance. In particular, define the sample mean $\hat{\boldsymbol{\mu}} = n^{-1} \sum_{i=1}^n \mathbf{X}_i$, and the usual maximum likelihood estimator, the sample covariance $\hat{\Sigma} = \widehat{\text{cov}}[\text{vec}(\mathbf{X})] = n^{-1} \sum_{i=1}^n \{\text{vec}(\mathbf{X}_i) - \text{vec}(\hat{\boldsymbol{\mu}})\} \{\text{vec}(\mathbf{X}_i) - \text{vec}(\hat{\boldsymbol{\mu}})\}^\top$. Although the sample covariance $\hat{\Sigma}$ is well-behaved for fixed p and q , it has undesired issues when $pq > n$. In particular, the sample covariance matrix is singular, and it may not be a consistent estimator of Σ^* . In addition, the eigenvalues are often overdispersed and may be inconsistent (Bickel and Levina, 2008a,b).

Therefore, to estimate Σ^* in high dimensional settings, we impose an additional assumption that the covariance of $\text{vec}(\mathbf{X})$ is separable, i.e.

$$\Sigma^* = \Sigma_2^* \otimes \Sigma_1^* \in \mathcal{S}_+^{pq \times pq},$$

where $\Sigma_1^* \in \mathcal{S}_+^{p \times p}$ and $\Sigma_2^* \in \mathcal{S}_+^{q \times q}$ represent covariances among the rows and columns of the matrices, respectively. The separability assumption provides a stable and parsimonious alternative to an unrestricted version of Σ^* , and reduces the number of parameters from $pq(pq + 1)/2$ to $(p(p + 1)/2 + q(q + 1)/2)$. This assumption is commonly used in modeling matrix-valued data (Dawid, 1981; Fuentes, 2006; Lu and Zimmerman, 2005; Mitchell et al., 2006; Hoff, 2011). However, when $p > n$ or $q > n$, the covariance estimates for Σ_1^* and Σ_2^* are still singular.

2.1 Bandable Covariance

To estimate the covariance matrix when $p > n$ or $q > n$, regularizing large empirical covariance matrices has been widely used in literature (Bickel and Levina, 2008b). One popular way is to band the sample covariance matrix. For any $\mathbf{A} = [A_{l,m}]_{d \times d}$, define

$$\mathcal{B}_d(k) = \{\mathbf{A} \in \mathbb{R}^{d \times d} : A_{l,m} = 0 \text{ for any } |l - m| > k, 1 \leq l, m \leq d\},$$

and

$$B_k(\mathbf{A}) = [A_{l,m} \cdot \mathbf{I}(|l - m| \leq k)]_{d \times d}.$$

We propose to solve the following optimization problem for a given pair of tuning parameters (k_1, k_2) :

$$(\widehat{\Sigma}_1^{\mathcal{B}}(k_1), \widehat{\Sigma}_2^{\mathcal{B}}(k_2)) = \underset{\Sigma_1 \in \mathcal{B}_p(k_1), \Sigma_2 \in \mathcal{B}_q(k_2)}{\operatorname{argmin}} \left\| \widehat{\Sigma} - \Sigma_2 \otimes \Sigma_1 \right\|_{\mathbb{F}}^2. \quad (2.1)$$

And the banded covariance estimate corresponding to (k_1, k_2) is $\widehat{\Sigma}^{\mathcal{B}}(k_1, k_2) = \widehat{\Sigma}_2^{\mathcal{B}}(k_2) \otimes \widehat{\Sigma}_1^{\mathcal{B}}(k_1)$. Here k_1 and k_2 control the regularization level of banding.

Surprisingly, the above problem has a closed form solution. Define $\widetilde{\Sigma}_{\mathcal{B}}(k_1, k_2)$ to be a $pq \times pq$ matrix satisfying $\widetilde{\Sigma}_{\mathcal{B}}(k_1, k_2) = \widehat{\Sigma} \circ \{B_{k_2}(\mathbf{1}_q) \otimes B_{k_1}(\mathbf{1}_p)\}$, where $\mathbf{1}_p$ and $\mathbf{1}_q$ are matrices of all 1's with dimension $p \times p$ and $q \times q$ respectively. We call $\widetilde{\Sigma}_{\mathcal{B}}(k_1, k_2)$ a doubly banded matrix of $\widehat{\Sigma}$ with bandwidths k_1 and k_2 . We have the following proposition whose proof is deferred to the Supplementary File.

Proposition 2.1. Solving (2.1) is equivalent to solving the following optimization problem

$$(\widehat{\Sigma}_1^{\mathcal{B}}(k_1), \widehat{\Sigma}_2^{\mathcal{B}}(k_2)) = \underset{\Sigma_1, \Sigma_2}{\operatorname{argmin}} \left\| \widetilde{\Sigma}_{\mathcal{B}}(k_1, k_2) - \Sigma_2 \otimes \Sigma_1 \right\|_{\mathbb{F}}^2. \quad (2.2)$$

This proposition provides an efficient way to solve the optimization problem (2.1). In particular, one can first obtain $\widetilde{\Sigma}_{\mathcal{B}}(k_1, k_2)$ by doubly banding $\widehat{\Sigma}$, and then solve the rank one unconstrained Kronecker product approximation (2.2) (Van Loan and Pitsianis, 1993; Pitsianis, 1997).

For completeness, we briefly introduce how to solve a general rank one unconstrained Kronecker product approximation problem. Suppose we have matrices $\mathbf{A} \in \mathbb{R}^{p_A \times q_A}$, $\mathbf{B} \in \mathbb{R}^{p_B \times q_B}$ and $\mathbf{C} \in \mathbb{R}^{p_C \times q_C}$ with $p_A = p_B p_C$ and $q_A = q_B q_C$. The goal is to solve

$$\min_{\mathbf{B}, \mathbf{C}} \left\| \mathbf{A} - \mathbf{B} \otimes \mathbf{C} \right\|_{\mathbb{F}}^2. \quad (2.3)$$

For a $p_B p_C \times q_B q_C$ matrix \mathbf{A} with submatrix structure,

$$\mathbf{A} = \begin{bmatrix} \mathbf{A}_{1,1} & \cdots & \mathbf{A}_{1,q_B} \\ \vdots & & \vdots \\ \mathbf{A}_{p_B,1} & \cdots & \mathbf{A}_{p_B,q_B} \end{bmatrix}$$

where the submatrix $\mathbf{A}_{i,j} \in \mathbb{R}^{p_C \times q_C}$. We define a matrix transformation $\xi(\cdot) : \mathbb{R}^{p_B p_C \times q_B q_C} \longrightarrow \mathbb{R}^{p_B q_B \times p_C q_C}$ as,

$$\xi(\mathbf{A}) = \begin{bmatrix} \text{vec}(\mathbf{A}_{1,1})^\top \\ \vdots \\ \text{vec}(\mathbf{A}_{q,1})^\top \\ \vdots \\ \text{vec}(\mathbf{A}_{q,q})^\top \end{bmatrix}. \quad (2.4)$$

Van Loan and Pitsianis (1993); Pitsianis (1997) showed that solving (2.3) is equivalent to solving a rank one singular value decomposition (SVD) of $\xi(\mathbf{A})$. In particular, they have shown the following propositions.

Proposition 2.2. $\|\mathbf{A} - \mathbf{B} \otimes \mathbf{C}\|_{\mathbb{F}}^2 = \|\xi(\mathbf{A}) - \mathbf{bc}^\top\|_{\mathbb{F}}^2$, where $\mathbf{b} = \text{vec}(\mathbf{B})$ and $\mathbf{c} = \text{vec}(\mathbf{C})$.

Proposition 2.3. The minimizer of $\min_{\mathbf{b}, \mathbf{c}} \|\xi(\mathbf{A}) - \mathbf{bc}^\top\|_{\mathbb{F}}^2$ is the same as the minimizer of $\min_{\mathbf{b}, \mathbf{c}} \|\xi(\mathbf{A}) - \mathbf{bc}^\top\|_2$.

By Propositions 2.2 and 2.3, solving (2.3) is equivalent to solving

$$\min_{\mathbf{b}, \mathbf{c}} \|\xi(\mathbf{A}) - \mathbf{bc}^\top\|_2. \quad (2.5)$$

Proposition 2.4. If the SVD of matrix $\xi(\mathbf{A}) = \mathbf{USV}$, where $\mathbf{U} \in \mathbb{R}^{p_A \times p_A}$ and $\mathbf{V} \in \mathbb{R}^{q_A \times q_A}$, and σ_1 is the largest singular value. Then the minimizer of (2.5) would be $\hat{\mathbf{b}} = C\sigma_1\mathbf{u}_1$ and $\hat{\mathbf{c}} = C^{-1}\mathbf{v}_1$ for any constant $C \neq 0$, where \mathbf{u}_1 and \mathbf{v}_1 are the first columns of matrices \mathbf{U} and \mathbf{V} .

The propositions 2.2, 2.3 and 2.4 are directly taken from Pitsianis (1997); Golub and VanLoan (1996), so we omit the proof. From these propositions, one can easily obtain the following proposition.

Proposition 2.5. The Kronecker approximation $\mathbf{B} \otimes \mathbf{C}$ is unique. In addition, if $(\mathbf{B}^*, \mathbf{C}^*)$ is a solution of (2.3), $(c\mathbf{B}^*, c^{-1}\mathbf{C}^*)$ is also a solution of (2.3) for any constant $c \neq 0$.

Proposition 2.5 implies that our banded covariance estimate $\widehat{\Sigma}^{\mathcal{B}}(k_1, k_2)$ is unique.

To implement the rank one unconstrained Kronecker product approximation, we adopt the algorithm proposed in [Batselier and Wong \(2017\)](#). The algorithm is implemented using the Matlab package TKPSVD, which can be downloaded at <https://github.com/kbatseli/TKPSVD>.

There are two tuning parameters k_1 and k_2 involved in our estimation procedure. Theoretically, we will show in Section 3 that when k_1 and k_2 are chosen appropriately, our estimator will be consistent even when both p and q diverge at the exponential order of the sample size n . In practice, we apply the resampling scheme procedure proposed in [Bickel and Levina \(2008b\)](#) to select the optimal bandwidths k_1 and k_2 . In particular, we randomly split the original sample into a training set and a testing set, with sample sizes n_1 and $n_2 = n - n_1$, respectively. We use the training sample to estimate the covariance matrix $\widehat{\Sigma}^{ta}(k_1, k_2)$ using our procedure, and compare with the sample covariance matrix of the test sample $\widehat{\Sigma}^{te}$. We repeat the random split procedure for N times, and let $\widehat{\Sigma}_\nu^{ta}(k_1, k_2)$ and $\widehat{\Sigma}_\nu^{te}$ denote the estimates from the ν th split with $\nu = 1, \dots, N$. We select the (k_1, k_2) that minimizes the following quantity

$$R(k_1, k_2) = N^{-1} \sum_{\nu=1}^N \|\widehat{\Sigma}_\nu^{ta}(k_1, k_2) - \widehat{\Sigma}_\nu^{te}\|_1.$$

Similar to [Bickel and Levina \(2008b\)](#), we choose $n_1 = \lfloor \frac{n}{3} \rfloor$ and $n_2 = n - n_1$. For the number of random split, we use $N = 10$ throughout the paper. Denote \widehat{k}_1 and \widehat{k}_2 as selected optimal bandwidths, our final banded covariance estimate is $\widehat{\Sigma}^{\mathcal{B}}(\widehat{k}_1, \widehat{k}_2) = \widehat{\Sigma}_2^{\mathcal{B}}(\widehat{k}_2) \otimes \widehat{\Sigma}_1^{\mathcal{B}}(\widehat{k}_1)$, where

$$(\widehat{\Sigma}_1^{\mathcal{B}}(\widehat{k}_1), \widehat{\Sigma}_2^{\mathcal{B}}(\widehat{k}_2)) = \underset{\Sigma_1 \in \mathcal{B}_p(\widehat{k}_1), \Sigma_2 \in \mathcal{B}_q(\widehat{k}_2)}{\operatorname{argmin}} \|\widehat{\Sigma} - \Sigma_2 \otimes \Sigma_1\|_{\mathbb{F}}^2.$$

2.2 Tapering Covariance

Another popular technique for covariance matrix regularization is tapering ([Bickel and Levina, 2008b](#); [Cai et al., 2010](#)). For any matrix $\mathbf{A} = [A_{l,m}]_{d \times d}$ and any $0 \leq k \leq$

d , we define $T_k(\mathbf{A}) = [T_k(\mathbf{A})_{l,m}]_{d \times d}$ where

$$T_k(\mathbf{A})_{l,m} = \begin{cases} A_{l,m} & \text{when } |l - m| \leq \lfloor k/2 \rfloor, \\ (2 - \frac{|l-m|}{\lfloor k/2 \rfloor})A_{l,m} & \text{when } \lfloor k/2 \rfloor < |l - m| \leq k, \\ 0 & \text{otherwise.} \end{cases} \quad (2.6)$$

Consider

$$\tilde{\Sigma}_{\mathcal{J}}(k_1, k_2) = \hat{\Sigma} \circ \{T_{k_2}(\mathbf{1}_q) \otimes T_{k_1}(\mathbf{1}_p)\}.$$

Analogous to (2.2), we propose to solve

$$(\hat{\Sigma}_1^{\mathcal{J}}(k_1), \hat{\Sigma}_2^{\mathcal{J}}(k_2)) = \underset{\Sigma_1, \Sigma_2}{\operatorname{argmin}} \|\tilde{\Sigma}_{\mathcal{J}}(k_1, k_2) - \Sigma_2 \otimes \Sigma_1\|_{\text{F}}^2. \quad (2.7)$$

Then we obtain the tapering covariance estimate as $\hat{\Sigma}^{\mathcal{J}}(k_1, k_2) = \hat{\Sigma}_2^{\mathcal{J}}(k_2) \otimes \hat{\Sigma}_1^{\mathcal{J}}(k_1)$.

For solving (2.7) and selecting the tapering tuning parameters (k_1, k_2) , we adopt the same resampling procedure as the one proposed for the banded estimate in Section 2.1.

3 Theoretical Results

3.1 Notation

Recall $\mathbf{X}_1, \dots, \mathbf{X}_n$, are i.i.d. $p \times q$ random matrix samples and $\operatorname{vec}(\mathbf{X}_i) \in \mathbb{R}^{pq}$ their vectorizations. For any $\mathbf{A} \in \mathbb{R}^{p \times q}$ and $\operatorname{vec}(\mathbf{A}) = (A_1, \dots, A_{pq})^{\text{T}}$, we define $A_{l_1, l_2} = A_{(l_2-1) \cdot p + l_1}$ as the $((l_2 - 1) \cdot p + l_1)$ th entry of $\operatorname{vec}(\mathbf{A})$ or, equivalently (l_1, l_2) th entry of \mathbf{A} . Denote $\operatorname{vec}(\mathbf{X}_i) = (x_1^i, \dots, x_{pq}^i)^{\text{T}}$ and x_{l_1, l_2}^i the (l_1, l_2) th entry of \mathbf{X}_i . Further define $\Sigma_1^* = [\sigma_{l_1, m_1}^{(1)}]_{p \times p}$, $\Sigma_2^* = [\sigma_{l_2, m_2}^{(2)}]_{q \times q}$, where $\sigma_{l_u, m_u}^{(u)}$ is the (l_u, m_u) th entry of Σ_u^* for $u = 1, 2$. We also define $\Sigma_u^{*,\beta}(k) = B_k(\Sigma_u^*)$ and $\Sigma_u^{*,\mathcal{J}}(k) = T_k(\Sigma_u^*)$ for $u = 1, 2$. For any matrix $\mathbf{A} = [A_{l,m}]_{pq \times pq} \in \mathbb{R}^{pq \times pq}$, let $A_{((l_1, m_1), (l_2, m_2))}$ represent the $((l_2 - 1) \cdot p + l_1, ((m_2 - 1) \cdot p + m_1))$ th entry of \mathbf{A} for $1 \leq l_1, m_1 \leq p, 1 \leq l_2, m_2 \leq q$. For $\Sigma^* \in \mathbb{R}^{pq \times pq}$, let $\sigma_{((l_1, m_1), (l_2, m_2))}$ be the $((l_2 - 1) \cdot p + l_1, ((m_2 - 1) \cdot p + m_1))$ th entry of Σ^* . By the separability assumption, one has $\Sigma^* = (\sigma_{((l_1, m_1), (l_2, m_2))}) = (\sigma_{l_1, m_1}^{(1)} \cdot \sigma_{l_2, m_2}^{(2)})$.

Denote \lesssim an inequality up to a multiplicative constant and \asymp an equality up to a multiplicative constant. Denote \mathcal{U}_{pq} a unit ball in \mathbb{R}^{pq} , and $\mathbf{1}_d$ a $d \times d$ matrix with all elements equal to 1.

Following [Bickel and Levina \(2008b\)](#), we define the following uniformity class of approximately bandable covariance matrices

$$\mathcal{F}(\varepsilon_0, \alpha) = \left\{ \boldsymbol{\Sigma} \geq 0 : \max_l \sum_m \{ |\sigma_{l,m}| : |l - m| > k \} \leq C_0 k^{-\alpha} \text{ for all } k \geq 0, \right. \\ \left. \text{and } 0 < \varepsilon_0 \leq \lambda_{\min}(\boldsymbol{\Sigma}) \leq \lambda_{\max}(\boldsymbol{\Sigma}) \leq 1/\varepsilon_0 \right\}, \quad (3.1)$$

with $\alpha > 0$. We further define another important class of covariance matrices ([Cai et al., 2010](#)),

$$\mathcal{M}(\varepsilon_0, \alpha) = \left\{ \boldsymbol{\Sigma} : |\sigma_{l,m}| \leq C_1 |l - m|^{-(\alpha+1)} \text{ for } l \neq m, \right. \\ \left. \text{and } 0 < \varepsilon_0 \leq \lambda_{\min}(\boldsymbol{\Sigma}) \leq \lambda_{\max}(\boldsymbol{\Sigma}) \leq 1/\varepsilon_0 \right\}. \quad (3.2)$$

One can see that $\mathcal{M}(\varepsilon_0, \alpha)$ is a subset of $\mathcal{F}(\varepsilon_0, \alpha)$ when $C_1 \leq \alpha C_0$. In other words, $\mathcal{M}(\varepsilon_0, \alpha)$ is a more restrictive class.

We say $\text{vec}(\mathbf{X})$ follows a sub-Gaussian distribution if for any $t > 0$ and $\|\mathbf{v}\| = 1$, there exists a $\rho > 0$ such that

$$\Pr \left\{ \left| \mathbf{v}^T \left(\text{vec}(\mathbf{X}) - \mathbb{E}(\text{vec}(\mathbf{X}_i)) \right) \right| > t \right\} \leq e^{-\rho t^2}, \quad (3.3)$$

3.2 Main Results

In this section, we present convergence rates of our banded/tapering covariance matrix estimates for two scenarios: (i) $\boldsymbol{\Sigma}_1^*$ and $\boldsymbol{\Sigma}_2^*$ are assumed in $\mathcal{F}(\varepsilon_0, \alpha)$; (ii) $\boldsymbol{\Sigma}_1^*$ and $\boldsymbol{\Sigma}_2^*$ are in a smaller class $\mathcal{M}(\varepsilon_0, \alpha)$. All the proofs are given in the Supplementary File.

Case (I): In parallel to [Bickel and Levina \(2008b\)](#), we consider the convergence rates of our covariance estimates when $\boldsymbol{\Sigma}_1^*$ and $\boldsymbol{\Sigma}_2^*$ reside in the uniformity class of approximately bandable covariance matrices $\mathcal{F}(\varepsilon_0, \alpha)$.

Let $\eta \in \{\mathcal{B}, \mathcal{T}\}$, and $\widehat{\Sigma}_2^\eta(k_2) \otimes \widehat{\Sigma}_1^\eta(k_1)$ denote either proposed banded or tapering estimator depending on the value of η . We present the following theorem for the proposed banded and tapering covariance estimators obtained from (2.1) and (2.7).

Theorem 3.1. Let $\text{vec}(\mathbf{X}_1), \text{vec}(\mathbf{X}_2), \dots, \text{vec}(\mathbf{X}_n)$ be i.i.d. sub-Gaussian random vectors in \mathbb{R}^{pq} with true covariance $\Sigma^* = \Sigma_2^* \otimes \Sigma_1^*$, where $\Sigma_1^* \in \mathcal{F}(\varepsilon_0, \alpha_1), \Sigma_2^* \in \mathcal{F}(\varepsilon_0, \alpha_2)$. And the row and coloum dimensions p, q satisfy $p, q \lesssim \exp(n)$.

(a) **High Dimensional Regime:** If p, q, n satisfy $\left(\frac{\log(\max(p, q))}{n}\right)^{-1} \lesssim p^{2\alpha_1+1} \cdot q^{2\alpha_2+1}$.

i. When $\alpha_2 \geq \alpha_1$, we have

$$\frac{\|\Sigma^* - \widehat{\Sigma}_2^\eta(k_2) \otimes \widehat{\Sigma}_1^\eta(k_1)\|_F}{\sqrt{pq}} = \begin{cases} \mathcal{O}_P\left(q^{-\frac{\alpha_2-\alpha_1}{2\alpha_1+1}} \cdot \left(\frac{\log(\max(p, q))}{n}\right)^{\frac{\alpha_1}{2\alpha_1+1}}\right) & \text{when } q \lesssim \left(\frac{\log(\max(p, q))}{n}\right)^{-\frac{1}{2\alpha_2+1}} \\ \mathcal{O}_P\left(\left(\frac{\log(\max(p, q))}{n}\right)^{\frac{\alpha_2}{2\alpha_2+1}}\right) & \text{when } q \gtrsim \left(\frac{\log(\max(p, q))}{n}\right)^{-\frac{1}{2\alpha_2+1}}, \end{cases} \quad (3.4)$$

$$\text{by taking } (k_1, k_2) = \begin{cases} \left(q^{-\frac{2\alpha_2+1}{2\alpha_1+1}} \cdot \left(\frac{\log(\max(p, q))}{n}\right)^{-\frac{1}{2\alpha_1+1}}, q\right) & \text{when } q \lesssim \left(\frac{\log(\max(p, q))}{n}\right)^{-\frac{1}{2\alpha_2+1}} \\ \left(1, \left(\frac{\log(\max(p, q))}{n}\right)^{-\frac{1}{2\alpha_2+1}}\right) & \text{when } q \gtrsim \left(\frac{\log(\max(p, q))}{n}\right)^{-\frac{1}{2\alpha_2+1}}. \end{cases}$$

ii. When $\alpha_2 \leq \alpha_1$, we have

$$\frac{\|\Sigma^* - \widehat{\Sigma}_2^\eta(k_2) \otimes \widehat{\Sigma}_1^\eta(k_1)\|_F}{\sqrt{pq}} = \begin{cases} \mathcal{O}_P\left(p^{-\frac{\alpha_1-\alpha_2}{2\alpha_2+1}} \cdot \left(\frac{\log(\max(p, q))}{n}\right)^{\frac{\alpha_2}{2\alpha_2+1}}\right) & \text{when } p \lesssim \left(\frac{\log(\max(p, q))}{n}\right)^{-\frac{1}{2\alpha_1+1}} \\ \mathcal{O}_P\left(\left(\frac{\log(\max(p, q))}{n}\right)^{\frac{\alpha_1}{2\alpha_1+1}}\right) & \text{when } p \gtrsim \left(\frac{\log(\max(p, q))}{n}\right)^{-\frac{1}{2\alpha_1+1}}, \end{cases} \quad (3.5)$$

$$\text{by taking } (k_1, k_2) = \begin{cases} \left(p, p^{-\frac{2\alpha_1+1}{2\alpha_2+1}} \cdot \left(\frac{\log(\max(p, q))}{n}\right)^{-\frac{1}{2\alpha_2+1}}\right) & \text{when } p \lesssim \left(\frac{\log(\max(p, q))}{n}\right)^{-\frac{1}{2\alpha_1+1}} \\ \left(\left(\frac{\log(\max(p, q))}{n}\right)^{-\frac{1}{2\alpha_1+1}}, 1\right) & \text{when } p \gtrsim \left(\frac{\log(\max(p, q))}{n}\right)^{-\frac{1}{2\alpha_1+1}}. \end{cases}$$

(b) **Low Dimensional Regime:** If p, q, n satisfy $\left(\frac{\log(\max(p, q))}{n}\right)^{-1} \gtrsim p^{2\alpha_1+1} \cdot q^{2\alpha_2+1}$, by taking $(k_1, k_2) = (p, q)$ when $\eta = \mathcal{B}$ and $(k_1, k_2) = (2p, 2q)$ when $\eta = \mathcal{T}$, we have

$$\frac{\|\Sigma^* - \widehat{\Sigma}_2^\eta(k_2) \otimes \widehat{\Sigma}_1^\eta(k_1)\|_F}{\sqrt{pq}} = \mathcal{O}_P\left(\left(pq \cdot \frac{\log(\max(p, q))}{n}\right)^{\frac{1}{2}}\right). \quad (3.6)$$

Under the **High Dimensional Regime** of Theorem 3.1, when $\alpha_2 \geq \alpha_1$ and q is fixed, the convergence rate of $\frac{\|\Sigma^* - \widehat{\Sigma}_2^\eta(k_2) \otimes \widehat{\Sigma}_1^\eta(k_1)\|_F}{\sqrt{pq}}$ is $\mathcal{O}_P\left(\frac{\log(\max(p, q))}{n}\right)^{\frac{\alpha_1}{2\alpha_1+1}}$. As q increases, the convergence rate is decreasing until q exceeds the order of $\left(\frac{\log(\max(p, q))}{n}\right)^{-\frac{1}{2\alpha_2+1}}$.

When q further increases, the convergence rate will remain at $\mathcal{O}_P\left(\frac{\log(\max(p,q))}{n}\right)^{\frac{\alpha_1}{2\alpha_2+1}}$.

When $\alpha_1 \geq \alpha_2$, one can observe a similar phenomenon. As such, under **High Dimensional Regime**, the convergence rate of $\frac{\|\Sigma^* - \widehat{\Sigma}_2^\eta(k_2) \otimes \widehat{\Sigma}_1^\eta(k_1)\|_F}{\sqrt{pq}}$ is within the range

$$\left[\left(\frac{\log(\max(p,q))}{n} \right)^{\frac{\max\{\alpha_1, \alpha_2\}}{2\max\{\alpha_1, \alpha_2\}+1}}, \left(\frac{\log(\max(p,q))}{n} \right)^{\frac{\min\{\alpha_1, \alpha_2\}}{2\min\{\alpha_1, \alpha_2\}+1}} \right].$$

Therefore, our result allows p and q diverging at the exponential order of sample size, i.e. $p, q = o(\exp(n))$.

Under the **Low Dimensional Regime** of Theorem 3.1, $\left(\frac{\log(\max(p,q))}{n}\right)^{-1} \gtrsim p^{2\alpha_1+1} q^{2\alpha_2+1}$ implies $\left(\frac{\log(\max(p,q))}{n}\right)^{-1} \gtrsim p^{2\min\{\alpha_1, \alpha_2\}+1} q^{2\min\{\alpha_1, \alpha_2\}+1}$ which shows

$$\begin{aligned} \frac{\|\Sigma^* - \widehat{\Sigma}_2^\eta(k_2) \otimes \widehat{\Sigma}_1^\eta(k_1)\|_F}{\sqrt{pq}} &= \mathcal{O}_P\left(\left(pq \frac{\log(\max(p,q))}{n}\right)^{\frac{1}{2}}\right) \\ &= \mathcal{O}_P\left(\left(\left(\frac{\log(\max(p,q))}{n}\right)^{-\frac{1}{2\min\{\alpha_1, \alpha_2\}}}\right) \cdot \left(\frac{\log(\max(p,q))}{n}\right)\right)^{1/2} \\ &= \mathcal{O}_P\left(\frac{\log(\max(p,q))}{n}\right)^{\frac{\min\{\alpha_1, \alpha_2\}}{2\min\{\alpha_1, \alpha_2\}+1}}. \end{aligned}$$

On the other side, the convergence rate we derive can never be faster than $n^{-1/2}$, which is attained when $(p, q) \asymp (1, 1)$.

Remark 3.2. When $q = 1$, our proposed banded/tapering estimators degenerate to Bickel's banded estimator/Cai's tapering estimator, i.e., $\widehat{\Sigma}^\eta(k_1)$. Therefore it makes sense to compare our convergence results with Bickel's banded estimator.

Under **High Dimensional Regime**, by (3.4) and (3.5), we have

$$\frac{\|\Sigma^* - \widehat{\Sigma}^\eta(k_1)\|_F}{\sqrt{p}} = \mathcal{O}_P\left(\left(\frac{\log(p)}{n}\right)^{\frac{\alpha_1}{2\alpha_1+1}}\right).$$

Under **Low Dimensional Regime**, $\left(\frac{\log(p)}{n}\right)^{-1} \gtrsim p^{2\alpha_1+1}$ implies $\left(\frac{\log(p)}{n}\right)^{-\frac{1}{2\alpha_1+1}} \gtrsim p$ and

$$\begin{aligned} \frac{\|\Sigma^* - \widehat{\Sigma}^\eta(k_1)\|_F}{\sqrt{p}} &= \mathcal{O}_P\left(\left(p \cdot \frac{\log(p)}{n}\right)^{1/2}\right) = \mathcal{O}_P\left(\left(\frac{\log(p)}{n}\right)^{\frac{1}{2} \cdot \left(-\frac{1}{2\alpha_1+1} + 1\right)}\right) \\ &= \mathcal{O}_P\left(\left(\frac{\log(p)}{n}\right)^{\frac{\alpha_1}{2\alpha_1+1}}\right). \end{aligned}$$

Therefore, $\frac{\|\Sigma^* - \widehat{\Sigma}^\eta(k_1)\|_F}{\sqrt{p}} = \mathcal{O}_P\left(\left(\frac{\log(p)}{n}\right)^{\frac{\alpha_1}{2\alpha_1+1}}\right)$ holds for both regimes. This rate is tighter compared to the convergence rate $\mathcal{O}_P\left(\left(\frac{\log(p)}{n}\right)^{-\frac{\alpha_1}{2\alpha_1+2}}\right)$ under the operator

norm as shown in [Bickel and Levina \(2008b\)](#). Intuitively this makes sense since for any $\mathbf{A} \in \mathbb{R}^{d \times d}$, we always have $\|\mathbf{A}\|_{\text{F}} \leq \sqrt{d}\|\mathbf{A}\|_2$. So the convergence rate of $\frac{\|\Sigma^* - \widehat{\Sigma}^\eta(k_1)\|_{\text{F}}}{\sqrt{p}}$ should be faster or equal to the convergence rate of $\|\Sigma^* - \widehat{\Sigma}^\eta(k_1)\|_2$.

Case (II): In parallel to [Cai et al. \(2010\)](#), we consider the convergence rate of our covariance estimates when Σ_1^* and Σ_2^* reside in a more restrictive class $\mathcal{M}_\alpha(\epsilon_0, \alpha)$. We have the following theorem which presents the convergence rate of the proposed banded and tapering covariance estimators obtained from [\(2.1\)](#) and [\(2.7\)](#).

Theorem 3.3. Let $\text{vec}(\mathbf{X}_1), \text{vec}(\mathbf{X}_2), \dots, \text{vec}(\mathbf{X}_n)$ be i.i.d random vectors in \mathbb{R}^{pq} with true covariance $\Sigma^* = \Sigma_2^* \otimes \Sigma_1^*$, where $\Sigma_1^* \in \mathcal{M}(\epsilon_0, \alpha_1), \Sigma_2^* \in \mathcal{M}(\epsilon_0, \alpha_2)$. Assume $\mathbb{E}[\{\text{vec}(\mathbf{X}_i)\}^{\text{T}} \mathbf{u}]^2 < +\infty$ for any $\mathbf{u} \in \mathcal{U}_{pq}$, we have

$$\begin{aligned} \frac{1}{pq} \mathbb{E} \|\widehat{\Sigma}_2^\eta(k_2) \otimes \widehat{\Sigma}_1^\eta(k_1) - \Sigma^*\|_{\text{F}}^2 &\lesssim \min \left\{ n^{\frac{1}{2\alpha_1+2} + \frac{1}{2\alpha_2+2} - 1}, \frac{p}{n} \cdot n^{\frac{1}{2\alpha_2+2}}, \frac{q}{n} \cdot n^{\frac{1}{2\alpha_1+2}}, \frac{pq}{n} \right\} \\ &= \begin{cases} n^{\frac{1}{2\alpha_1+2} + \frac{1}{2\alpha_2+2} - 1} & \text{when } n^{\frac{1}{2\alpha_1+2}} \lesssim p, n^{\frac{1}{2\alpha_2+2}} \lesssim q \\ p \cdot n^{\frac{1}{2\alpha_2+2} - 1} & \text{when } p \lesssim n^{\frac{1}{2\alpha_1+2}}, n^{\frac{1}{2\alpha_2+2}} \lesssim q \\ q \cdot n^{\frac{1}{2\alpha_2+2} - 1} & \text{when } q \lesssim n^{\frac{1}{2\alpha_2+2}}, n^{\frac{1}{2\alpha_1+2}} \lesssim p \\ \frac{pq}{n} & \text{when } p \lesssim n^{\frac{1}{2\alpha_1+2}}, q \lesssim n^{\frac{1}{2\alpha_2+2}} \end{cases}. \end{aligned} \tag{3.7}$$

by choosing k_1, k_2 as

$$k_1 \asymp \begin{cases} n^{\frac{1}{2\alpha_1+2}} & \text{when } n^{\frac{1}{2\alpha_1+2}} \lesssim p \\ p & \text{when } p \lesssim n^{\frac{1}{2\alpha_1+2}} \end{cases}, k_2 \asymp \begin{cases} n^{\frac{1}{2\alpha_2+2}} & \text{when } n^{\frac{1}{2\alpha_2+2}} \lesssim q \\ q & \text{when } q \lesssim n^{\frac{1}{2\alpha_2+2}} \end{cases}.$$

In [Theorem 3.3](#) we derive the \mathcal{L}^2 convergence rate of our proposed estimators under Frobenius norm when Σ_1^*, Σ_2^* belong to smaller classes $\mathcal{M}(\epsilon_0, \alpha_1), \mathcal{M}(\epsilon_0, \alpha_2)$. By Markov's inequality, the \mathcal{L}^2 convergence rate in [\(3.7\)](#) implies the same convergence rate in probability.

It is easy to see that the convergence rate is bounded above by $C n^{\frac{1}{2\alpha_1+2} + \frac{1}{2\alpha_2+2} - 1}$ for some constant $C > 0$. Therefore, $\frac{1}{pq} \mathbb{E} \|\widehat{\Sigma}_2^\eta(k_2) \otimes \widehat{\Sigma}_1^\eta(k_1) - \Sigma^*\|_{\text{F}}^2$ always converges when $n \rightarrow +\infty$ regardless of the values for p, q .

Remark 3.4. When $q = 1$, our proposed estimators degenerate to Bickel's banded estimators/Cai's tapering estimators and it can be easily seen that

$$\min \left\{ \frac{q}{n} \cdot n^{\frac{1}{2\alpha_1+2}}, n^{\frac{1}{2\alpha_1+2} + \frac{1}{2\alpha_2+2} - 1} \right\} = n^{-(2\alpha_1+1)/2(\alpha_1+1)} \quad \text{and} \quad \min \left\{ \frac{p}{n} \cdot n^{\frac{1}{2\alpha_2+2}}, \frac{pq}{n} \right\} = \frac{p}{n}.$$

So the convergence rate of $\frac{1}{p} \mathbb{E} \|\widehat{\Sigma}_1^\eta(k_1) - \Sigma^*\|_{\mathbb{F}}^2$ is $\min \left\{ n^{-(2\alpha_1+1)/2(\alpha_1+1)}, \frac{p}{n} \right\}$, which coincides with the optimal \mathcal{L}^2 convergence rate proposed in Cai's tapering estimator shown in Theorem 4 of Cai et al. (2010).

Remark 3.5. In Theorem 3.3, we do not require the sub-Gaussian assumption as that in Theorem 3.1, and we only need a boundness assumption of the second moments. The trade-off is that we need to restrict Σ_1^* and Σ_2^* to smaller classes $\mathcal{M}(\epsilon_0, \alpha_1)$ and $\mathcal{M}(\epsilon_0, \alpha_2)$.

Remark 3.6. Under the degenerated scenario, i.e. when p or q is equal to 1, Cai et al. (2010) shows that Theorem 3.1 gives the \mathcal{L}^2 optimal convergence rate under Frobenius norm. Further Theorem 3.3 also shows a better convergence rate in probability compared with the rate in Theorem 3.1 when Σ_1^* or Σ_2^* is restricted in $\mathcal{M}(\epsilon_0, \alpha_1)$ or $\mathcal{M}(\epsilon_0, \alpha_2)$.

However, for general p and q , Theorem 3.3 does not always imply a better convergence rate in probability for general matrix-valued data compared with that in Theorem 3.1. Consider a specific condition when $(p, q) \asymp n^2, \alpha_2 \geq \alpha_1$ and $\Sigma_1^* \in \mathcal{M}(\epsilon_0, \alpha_1), \Sigma_2^* \in \mathcal{M}(\epsilon_0, \alpha_2)$. It follows that

$$p \asymp n^2 \gtrsim \left(\frac{\log(\max(p, q))}{n} \right)^{-\frac{1}{2\alpha_1+1}} \gtrsim n^{\frac{1}{2\alpha_1+2}}, q \asymp n^2 \gtrsim \left(\frac{\log(\max(p, q))}{n} \right)^{-\frac{1}{2\alpha_2+1}} \gtrsim n^{\frac{1}{2\alpha_2+2}}.$$

So Theorem 3.1 shows the convergence rate of $\frac{\|\Sigma^* - \widehat{\Sigma}_2^\eta(k_2) \otimes \widehat{\Sigma}_1^\eta(k_1)\|_{\mathbb{F}}}{\sqrt{pq}}$ is

$$\mathcal{O}_P \left(\left(\frac{\log(\max(p, q))}{n} \right)^{\frac{\alpha_2}{2\alpha_2+1}} \right) = \mathcal{O}_P \left(\left(\frac{\log(n)}{n} \right)^{\frac{\alpha_2}{2\alpha_2+1}} \right) = \mathcal{O}_P \left((\log n)^{\frac{\alpha_2}{2\alpha_2+1}} (n)^{-\frac{\alpha_2}{(2\alpha_2+1)}} \right)$$

and Theorem 3.3 shows the convergence rate in probability is

$$\mathcal{O}_P \left(n^{\frac{1}{2} \left(\frac{1}{2\alpha_2+2} + \frac{1}{2\alpha_1+2} - 1 \right)} \right) = \mathcal{O}_P \left(n^{-\frac{2\alpha_1\alpha_2 + \alpha_1 + \alpha_2}{4(\alpha_1+1)(\alpha_2+1)}} \right).$$

With simple algebra, we could see that $-\frac{\alpha_2}{(2\alpha_2+1)}$ is strictly smaller than $-\frac{2\alpha_1\alpha_2 + \alpha_1 + \alpha_2}{4(\alpha_1+1)(\alpha_2+1)}$.

So the convergence rate shown in Theorem 3.1 is strictly faster than the rate shown in Theorem 3.3. We have also included a more detailed comparison of the rates between Theorem 3.1 and Theorem 3.3 in the Supplementary File, Section 1.

4 Robust Covariance Estimation

Theorem 3.1 is based on the assumption that $\text{vec}(\mathbf{X}_i)$'s have sub-Gaussian tails. However, this assumption is often violated in practice. For example, financial returns and macroeconomic variables show heavy-tailed phenomenon (Cont (2001)); while many biological datasets also exhibit heavy tails, e.g., histogram distribution of intensity for brain tissue (Castillo-Barnes et al. (2017)), fluctuated microarray data (Liu et al. (2003), Purdom and Holmes (2005)).

To deal with potential heavy-tailed data, we propose a robust procedure to obtain banded/tapering covariance estimates. In particular, we adopt the idea in Fan et al. (2016) and truncate the sample covariance as a preliminary step. When $\text{vec}(\mathbf{X}_i) \in \mathbb{R}^{pq}$, the modified estimator is defined as

$$\check{\Sigma} = \frac{1}{n} \sum_{i=1}^n \text{vec}(\check{\mathbf{X}}_i) \cdot \text{vec}(\check{\mathbf{X}}_i)^\top,$$

where $\text{vec}(\check{\mathbf{X}}_i)$ satisfies $\check{x}_{l_1, l_2}^i = \text{sgn}(x_{l_1, l_2}^i)(|x_{l_1, l_2}^i| \wedge \tau)$ and $\tau \asymp (\log(\max(p, q))/n)^{-1/4}$. Fan et al. (2016) shows that if $\mathbb{E}(\text{vec}(\mathbf{X}_i)) = \mathbf{0}$ and $\mathbb{E}[\{\text{vec}(\mathbf{X}_i)\}^\top \mathbf{u}]^4 < +\infty$ for any $\mathbf{u} \in \mathcal{U}_{pq}$, then

$$\|\check{\Sigma} - \Sigma^*\|_\infty = \mathcal{O}_P(\sqrt{\log \max(p, q)/n}).$$

Therefore, instead of using the sample covariance $\hat{\Sigma}$, we replace $\hat{\Sigma}$ with $\check{\Sigma}$ when implementing our banded and/or tapering estimation procedure. In particular, define

$$\check{\Sigma}_{\mathcal{B}}(k_1, k_2) = \check{\Sigma} \circ \{B_{k_2}(\mathbf{1}_q) \otimes B_{k_1}(\mathbf{1}_p)\}, \check{\Sigma}_{\mathcal{T}}(k_1, k_2) = \check{\Sigma} \circ \{T_{k_2}(\mathbf{1}_q) \otimes T_{k_1}(\mathbf{1}_p)\}$$

as the banded/tapering matrix of $\check{\Sigma}$ with parameters k_1 and k_2 . We propose the robust banded/tapering estimators as $\hat{\Sigma}^{\mathcal{R}, \eta}(k_1, k_2) = \hat{\Sigma}_2^{\mathcal{R}, \eta}(k_2) \otimes \hat{\Sigma}_1^{\mathcal{R}, \eta}(k_1)$, where $\eta \in \{\mathcal{B}, \mathcal{T}\}$ and $\hat{\Sigma}_1^{\mathcal{R}, \eta}(k_1), \hat{\Sigma}_2^{\mathcal{R}, \eta}(k_2)$ are solutions from

$$(\hat{\Sigma}_1^{\mathcal{R}, \eta}(k_1), \hat{\Sigma}_2^{\mathcal{R}, \eta}(k_2)) = \underset{\Sigma_1, \Sigma_2}{\text{argmin}} \|\check{\Sigma}_\eta(k_1, k_2) - \Sigma_2 \otimes \Sigma_1\|_{\text{F}}^2. \quad (4.1)$$

We can show that our modified robust estimator achieves the same convergence rate as the one obtained from our original banded or tapering estimator designed for sub-Gaussian data, when p, q diverge at the exponential order of the sample

size. The result is given in the following theorem; and the proof is included in the Supplementary File.

Theorem 4.1. Let $\text{vec}(\mathbf{X}_1), \text{vec}(\mathbf{X}_2), \dots, \text{vec}(\mathbf{X}_n)$ be i.i.d random vectors in \mathbb{R}^{pq} with true covariance $\Sigma^* = \Sigma_2^* \otimes \Sigma_1^*$, where $\Sigma_1^* \in \mathcal{F}(\varepsilon_0, \alpha_1)$, and $\Sigma_2^* \in \mathcal{F}(\varepsilon_0, \alpha_2)$. Assume $\mathbb{E}(\text{vec}(\mathbf{X}_i)) = 0$ and $\mathbb{E}[\{\text{vec}(\mathbf{X}_i)\}^T \mathbf{u}]^4 < +\infty$ for any $\mathbf{u} \in \mathcal{U}_{pq}$ and $p, q \lesssim \exp(n)$.

(a) **High Dimensional Regime:** If p, q, n satisfy $\left(\frac{\log(\max(p, q))}{n}\right)^{-1} \lesssim p^{2\alpha_1+1} \cdot q^{2\alpha_2+1}$.

i. When $\alpha_2 \geq \alpha_1$, we have

$$\frac{\|\Sigma^* - \widehat{\Sigma}_2^{\mathcal{R}, \eta}(k_2) \otimes \widehat{\Sigma}_1^{\mathcal{R}, \eta}(k_1)\|_{\text{F}}}{\sqrt{pq}} = \begin{cases} \mathcal{O}_P\left(q^{-\frac{\alpha_2 - \alpha_1}{2\alpha_1 + 1}} \cdot \left(\frac{\log(\max(p, q))}{n}\right)^{\frac{\alpha_1}{2\alpha_1 + 1}}\right) & \text{when } q \lesssim \left(\frac{\log(\max(p, q))}{n}\right)^{-\frac{1}{2\alpha_2 + 1}} \\ \mathcal{O}_P\left(\left(\frac{\log(\max(p, q))}{n}\right)^{\frac{\alpha_2}{2\alpha_2 + 1}}\right) & \text{when } q \gtrsim \left(\frac{\log(\max(p, q))}{n}\right)^{-\frac{1}{2\alpha_2 + 1}}, \end{cases}$$

$$\text{by taking } (k_1, k_2) = \begin{cases} \left(q^{-\frac{2\alpha_2 + 1}{2\alpha_1 + 1}} \cdot \left(\frac{\log(\max(p, q))}{n}\right)^{-\frac{1}{2\alpha_1 + 1}}, q\right) & \text{when } q \lesssim \left(\frac{\log(\max(p, q))}{n}\right)^{-\frac{1}{2\alpha_2 + 1}} \\ \left(1, \left(\frac{\log(\max(p, q))}{n}\right)^{-\frac{1}{2\alpha_2 + 1}}\right) & \text{when } q \gtrsim \left(\frac{\log(\max(p, q))}{n}\right)^{-\frac{1}{2\alpha_2 + 1}} \end{cases}$$

and $\tau = (\log(\max(p, q))/n)^{-1/4}$.

ii. When $\alpha_2 \leq \alpha_1$, we have

$$\frac{\|\Sigma^* - \widehat{\Sigma}_2^{\mathcal{R}, \eta}(k_2) \otimes \widehat{\Sigma}_1^{\mathcal{R}, \eta}(k_1)\|_{\text{F}}}{\sqrt{pq}} = \begin{cases} \mathcal{O}_P\left(p^{-\frac{\alpha_1 - \alpha_2}{2\alpha_2 + 1}} \cdot \left(\frac{\log(\max(p, q))}{n}\right)^{\frac{\alpha_2}{2\alpha_2 + 1}}\right) & \text{when } p \lesssim \left(\frac{\log(\max(p, q))}{n}\right)^{-\frac{1}{2\alpha_1 + 1}} \\ \mathcal{O}_P\left(\left(\frac{\log(\max(p, q))}{n}\right)^{\frac{\alpha_1}{2\alpha_1 + 1}}\right) & \text{when } p \gtrsim \left(\frac{\log(\max(p, q))}{n}\right)^{-\frac{1}{2\alpha_1 + 1}}, \end{cases}$$

$$\text{by taking } (k_1, k_2) = \begin{cases} \left(p, p^{-\frac{2\alpha_1 + 1}{2\alpha_2 + 1}} \cdot \left(\frac{\log(\max(p, q))}{n}\right)^{-\frac{1}{2\alpha_2 + 1}}\right) & \text{when } p \lesssim \left(\frac{\log(\max(p, q))}{n}\right)^{-\frac{1}{2\alpha_1 + 1}} \\ \left(\left(\frac{\log(\max(p, q))}{n}\right)^{-\frac{1}{2\alpha_1 + 1}}, 1\right) & \text{when } p \gtrsim \left(\frac{\log(\max(p, q))}{n}\right)^{-\frac{1}{2\alpha_1 + 1}} \end{cases}$$

and $\tau = (\log(\max(p, q))/n)^{-1/4}$

(b) **Low Dimensional Regime:** If p, q, n satisfy $\left(\frac{\log(\max(p, q))}{n}\right)^{-1} \gtrsim p^{2\alpha_1+1} \cdot q^{2\alpha_2+1}$, by taking $(k_1, k_2) = (p, q)$ when $\eta = \mathcal{B}$ and $(k_1, k_2) = (2p, 2q)$ when $\eta = \mathcal{T}$, and taking $\tau = (\log(\max(p, q))/n)^{-1/4}$, we have

$$\frac{\|\Sigma^* - \widehat{\Sigma}_2^{\mathcal{R}, \eta}(k_2) \otimes \widehat{\Sigma}_1^{\mathcal{R}, \eta}(k_1)\|_{\text{F}}}{\sqrt{pq}} = \mathcal{O}_P\left(\left(pq \cdot \frac{\log(\max(p, q))}{n}\right)^{\frac{1}{2}}\right).$$

Remark 4.2. Unlike the banded/tapering estimator proposed in Section 2, the modified robust banded/tapering estimator relies on the assumption that $\mathbb{E}(\text{vec}(\mathbf{X}_i)) = 0$.

If this does not hold, we can newly define $\tilde{\mathbf{X}}_i = \frac{n}{n-1} \cdot (\mathbf{X}_i - \bar{\mathbf{X}})$, and estimate $\check{\Sigma}$ based on $\text{vec}(\tilde{\mathbf{X}}_i)$'s. It is easy to check

$$\mathbb{E}[\{\text{vec}(\tilde{\mathbf{X}}_i)\}^T \mathbf{u}]^4 < +\infty \text{ for any } \mathbf{u} \in \mathcal{U}_{pq},$$

and $\tilde{\mathbf{X}}_i$ satisfying $\mathbb{E}\tilde{\mathbf{X}}_i = \mathbf{0}$, and $\text{cov}(\tilde{\mathbf{X}}_i) = \Sigma^*$. Then we can apply our robust procedure to $\text{vec}(\tilde{\mathbf{X}}_i)$ directly.

Remark 4.3. Surprisingly, Theorem 4.1 shows that if we replace $\hat{\Sigma}$ with $\check{\Sigma}$ in our proposed procedures, we can attain the same convergence rate presented in Theorem 3.1 without the sub-Gaussian assumption. Technically speaking, entrywisely we can control the max norm difference $\|\hat{\Sigma} - \Sigma^*\|_{\max}$ with $\mathcal{O}_P\left(\left(\frac{\log(\max(p,q))}{n}\right)^{1/2}\right)$ for sub-Gaussian data. However, this is no longer true for heavy-tailed data. Surprisingly, by replacing $\hat{\Sigma}$ with $\check{\Sigma}$, the gap can be bridged as $\check{\Sigma}$ has a better statistical error control under max norm, i.e. $\|\check{\Sigma} - \Sigma^*\|_{\max} = \left(\frac{\log(\max(p,q))}{n}\right)^{1/2}$. In fact, Fan et al. (2016) shows that shrinkage estimator can actually outperform the classical estimator even for sub-Gaussian data. Therefore, replacing $\hat{\Sigma}$ with $\check{\Sigma}$ in our procedure will not affect the convergence rate even for sub-Gaussian data.

Remark 4.4. Although in Theorem 3.3, we do not require sub-Gaussian assumption either, the trade-off is that we need to restrict Σ_1^* and Σ_2^* to smaller classes $\mathcal{M}(\epsilon_0, \alpha_1)$ and $\mathcal{M}(\epsilon_0, \alpha_2)$. In addition, the rates in Theorem 4.1 may be faster than the convergence rate in probability implied by Theorem 3.3 even we restrict Σ_1^* and Σ_2^* to smaller classes $\mathcal{M}(\epsilon_0, \alpha_1)$ and $\mathcal{M}(\epsilon_0, \alpha_2)$.

Theoretically, we show that when $\tau = (\log(\max(p, q))/n)^{-1/4}$, our estimators can achieve the rates presented in Theorem 4.1. In practice, we adopt the resampling scheme in Section 2.1 to select τ from a candidate pool $\mathbb{T} = \{|x|_\iota : \iota \in \mathcal{P}\}$, where $|x|_\iota$ is the ι percentile value among the set of all possible absolute values of coordinates in any \mathbf{X}_i , i.e., $\{|x_{l_1, l_2}^i| : 1 \leq i \leq n, 1 \leq l_1 \leq p, 1 \leq l_2 \leq q\}$ and \mathcal{P} is a candidate pool of percentiles under consideration. To solve (4.1) and select the tuning parameters (k_1, k_2) , we adopt the same procedures as the ones used in non-robust banded/tapering covariance estimation in Section 2.1.

5 Simulation

5.1 Banded and Tapering Estimator

We investigate the finite sample performance of the proposed estimator by simulations. We first consider the case when the data are generated from multivariate normal distributions. In particular, the $\{\text{vec}(\mathbf{X}_i), 1 \leq i \leq n\}$ are i.i.d generated from $N(\mathbf{0}, \Sigma)$ with $\Sigma = \Sigma_2 \otimes \Sigma_1$, where $\Sigma_1 \in \mathbb{R}^{p \times p}$ and $\Sigma_2 \in \mathbb{R}^{q \times q}$. We consider the following two covariance structures for Σ_1 and Σ_2 .

Case 1. *Moving average covariance structure*

We set Σ_1 and Σ_2 to be the covariances of MA(1) process with

$$\begin{aligned}\sigma_{l_1, m_1}^{(1)} &= \rho_1^{|l_1 - m_1|} * \mathbf{1}\{|l_1 - m_1| \leq 1\}, \quad 1 \leq l_1, m_1 \leq p, \\ \sigma_{l_2, m_2}^{(2)} &= \rho_2^{|l_2 - m_2|} * \mathbf{1}\{|l_2 - m_2| \leq 1\}, \quad 1 \leq l_2, m_2 \leq q,\end{aligned}$$

where $\rho_1 = \rho_2 = 0.5$.

Case 2. *Autoregressive covariance structure*

We take Σ_1 and Σ_2 to be the covariances of AR(1) process with

$$\begin{aligned}\sigma_{l_1, m_1}^{(1)} &= \rho_1^{|l_1 - m_1|}, \quad 1 \leq l_1, m_1 \leq p, \\ \sigma_{l_2, m_2}^{(2)} &= \rho_2^{|l_2 - m_2|}, \quad 1 \leq l_2, m_2 \leq q,\end{aligned}$$

where we consider $(\rho_1, \rho_2) = (0.1, 0.1), (0.5, 0.5), (0.8, 0.8)$.

We consider $n = 50, 100, 200$, and $(p, q) = (20, 30), (100, 100)$. We compare our proposed estimators with the banded estimator of [Bickel and Levina \(2008b\)](#), the tapering estimator of [Cai et al. \(2010\)](#) and the sample covariance estimator. For the three comparison estimators, we directly estimate the corresponding covariance matrices from $\{\text{vec}(\mathbf{X}_i), 1 \leq i \leq n\}$ without using the Kronecker decomposition. We use the resampling scheme to choose the bandwidth for Bickel's banded estimator and Cai's tapering estimator. The random splits procedure is repeated for $N = 10$ times.

We report several quantities, $\|\widehat{\Sigma} - \Sigma\|_F$, $\|\widehat{\Sigma} - \Sigma\|_1$ and $\|\widehat{\Sigma} - \Sigma\|_2$, where $\widehat{\Sigma}$ can be our proposed estimators, Bickel's banded estimator, Cai's tapering estimator and

naive sample covariance estimator. These quantities characterize the estimation errors for the covariance matrices. We also report the \hat{k}_1 and \hat{k}_2 for our proposed methods and \hat{k} for [Bickel and Levina \(2008b\)](#)'s banded estimator and [Cai et al. \(2010\)](#)'s tapering estimator. We summarize the averages of these quantities over 100 Monte Carlo repetitions in [Tables 1 and 2](#) and [Tables S1-S4](#) in [Section 5.1](#) of the [Supplementary File](#). Their associated standard errors are summarized in [Section 5.2](#) of the [Supplementary File](#).

Table 1: Simulation results for $(p, q, \rho_1, \rho_2) = (100, 100, 0.5, 0.5)$ with the MA(1) covariance structure over 100 simulated replications. The averages of $\|\hat{\Sigma} - \Sigma\|_F$, $\|\hat{\Sigma} - \Sigma\|_1$ and $\|\hat{\Sigma} - \Sigma\|_2$ for the proposed estimators (Proposed B and Proposed T), Bickel's banded estimator (Banded), Cai's tapering estimator (Tapering) and the sample covariance estimator (Sample) are reported. The averages of \hat{k}_1 and \hat{k}_2 for the proposed banded and tapering estimators, the averages of \hat{k} for Bickel's banded estimator and Cai's tapering estimator are also reported.

$(n, p, q, \rho_1, \rho_2)$	Method	$\ \hat{\Sigma} - \Sigma\ _F$	$\ \hat{\Sigma} - \Sigma\ _1$	$\ \hat{\Sigma} - \Sigma\ _2$	\hat{k}	\hat{k}_1	\hat{k}_2
(50, 20, 30, 0.5, 0.5)	Sample	1428.40	1605.38	244.51			
	Banded	91.39	4.08	2.59	1.09		
	Tapering	93.40	4.49	2.80	2.00		
	Proposed B	8.41	0.79	0.49		1.73	1.87
	Proposed T	8.71	0.81	0.51		2.00	2.00
(100, 20, 30, 0.5, 0.5)	Sample	1004.87	1031.87	130.38			
	Banded	88.68	3.37	2.29	1.05		
	Tapering	89.76	3.63	2.42	2.00		
	Proposed B	5.85	0.53	0.33		1.65	1.84
	Proposed T	6.13	0.56	0.35		2.00	2.00
(200, 20, 30, 0.5, 0.5)	Sample	708.89	683.42	71.37			
	Banded	87.37	2.95	2.15	1.07		
	Tapering	87.93	3.14	2.22	2.08		
	Proposed B	4.16	0.38	0.23		1.79	1.82
	Proposed T	4.32	0.39	0.25		2.00	2.00

From these tables, we can see that our proposed methods always perform better than the comparison methods in terms of estimation errors. For Case 1, the oracle k_1 and k_2 for the banded estimator are both 1. Noticing that $B_1(\mathbf{1}_p) = T_2(\mathbf{1}_p)$, the

Table 2: Simulation results for $(p, q, \rho_1, \rho_2) = (100, 100, 0.1, 0.1)$ and $(p, q, \rho_1, \rho_2) = (100, 100, 0.5, 0.5)$ with AR(1) covariance structure over 100 replications. The averages of $\|\widehat{\Sigma} - \Sigma\|_F$, $\|\widehat{\Sigma} - \Sigma\|_1$ and $\|\widehat{\Sigma} - \Sigma\|_2$ for the proposed estimators (Proposed B and Proposed T), Bickel's banded estimator (Banded), Cai's tapering estimator (Tapering) and the sample covariance estimator (Sample) are reported. The averages of \widehat{k}_1 and \widehat{k}_2 for the proposed banded and tapering estimators, the averages of \widehat{k} for Bickel's banded estimator and Cai's tapering estimator are also reported.

$(n, p, q, \rho_1, \rho_2)$	Method	$\ \widehat{\Sigma} - \Sigma\ _F$	$\ \widehat{\Sigma} - \Sigma\ _1$	$\ \widehat{\Sigma} - \Sigma\ _2$	\widehat{k}	\widehat{k}_1	\widehat{k}_2
(50, 100, 100, 0.1, 0.1)	Sample	1428.38	1598.50	231.64			
	Banded	32.14	1.84	1.19	1.02		
	Tapering	29.33	1.53	1.03	1.09		
	Proposed B	6.16	0.36	0.20		2.37	2.28
	Proposed T	6.44	0.37	0.21		2.80	2.78
(100, 100, 100, 0.1, 0.1)	Sample	1004.94	1029.06	120.68			
	Banded	24.84	1.31	0.80	1.03		
	Tapering	25.03	1.19	0.72	1.11		
	Proposed B	4.25	0.26	0.14		2.78	2.49
	Proposed T	4.09	0.25	0.14		3.00	2.98
(200, 100, 100, 0.1, 0.1)	Sample	708.84	679.93	64.43			
	Banded	22.58	1.16	0.62	2.04		
	Tapering	22.49	1.15	0.62	2.00		
	Proposed B	3.41	0.24	0.11		4.44	4.38
	Proposed T	2.94	0.19	0.10		4.01	4.03
(50, 100, 100, 0.5, 0.5)	Sample	1428.37	1606.57	250.19			
	Banded	113.01	9.54	6.45	2.68		
	Tapering	112.91	9.50	6.46	2.96		
	Proposed B	19.27	3.20	1.46		5.30	5.11
	Proposed T	17.81	2.85	1.42		5.48	5.06
(100, 100, 100, 0.5, 0.5)	Sample	1005.05	1029.25	134.55			
	Banded	109.18	8.45	6.33	2.91		
	Tapering	109.11	8.40	6.33	3.32		
	Proposed B	13.69	2.47	1.07		6.65	6.43
	Proposed T	13.09	2.26	1.06		7.18	7.14
(200, 100, 100, 0.5, 0.5)	Sample	708.97	684.42	74.77			
	Banded	107.05	7.79	6.24	3.23		
	Tapering	106.94	7.73	6.23	3.88		
	Proposed B	10.32	1.70	0.80		5.52	5.29
	Proposed T	9.69	1.61	0.83		5.68	5.74

oracle k_1 and k_2 for the banded estimator are both 2, so our method can select \widehat{k}_1 and \widehat{k}_2 accurately. For Case 2, when ρ_1 and ρ_2 increase, the selected bandwidths \widehat{k}_1 and \widehat{k}_2 for the proposed method also increase, which is as expected.

5.2 Robust Banded and Tapering Estimators for Heavy-tailed Data

In this subsection, we investigate the finite sample performance of our proposed robust estimators when the data follow heavy-tailed distributions. In particular, we consider i.i.d. $p \times q$ matrix-valued data \mathbf{X}_i with $\text{vec}(\mathbf{X}_i)$ following multivariate t distributions with degree of freedom 3, i.e. $t_3(0, \Sigma)$ with $\Sigma = \Sigma_2 \otimes \Sigma_1$. Similar to Section 5.1, we consider two covariance structures. Case 1: Σ_1, Σ_2 are the covariances of MA(1) process, where we set $(p, q, \rho_1, \rho_2) = (20, 30, 0.5, 0.5)$ and $n = 50, 100, 200$. Case 2: Σ_1, Σ_2 are the covariances of AR(1) process, where we consider $(\rho_1, \rho_2) = (0.1, 0.1), (0.5, 0.5), (0.8, 0.8)$ and $(n, p, q) = (50, 20, 30)$.

We compare the proposed robust banded and tapering estimators with the non-robust version of banded and tapering estimators introduced in Section 2 as well as the sample covariance estimator. The results for both cases are summarized in Table S5 in the Supplementary File and Table 3 based on 100 Monte Carlo replications, respectively. We use the random splitting procedure introduced in Section 2.1 and Section 4 to select $\widehat{k}_1, \widehat{k}_2$ and choose the truncation threshold $\widehat{\tau}$ based on $\mathcal{P} = \{99.9999, 99.999, 99.99, 99.9, 95, 90\}$.

From the results, we can see the proposed robust estimators always outperform all the other methods. For Case 1 (Table S5), when n becomes larger, the selected $\widehat{\tau}$ for the proposed robust estimators decreases. For Case 2 (Table 3), we can see a clear improvement of estimation accuracy by adopting the robust covariance estimation as ρ_1, ρ_2 increase. Meanwhile, the selected bandwidths $\widehat{k}_1, \widehat{k}_2$ increase and the selected $\widehat{\tau}$ decreases as expected.

Table 3: Simulation results for heavy tail data with $(\rho_1, \rho_2) = (0.1, 0.1), (0.5, 0.5), (0.8, 0.8)$, $(n, p, q) = (50, 20, 30)$, and AR(1) covariance structure over 100 replications. The averages of $\|\widehat{\Sigma} - \Sigma\|_F$, $\|\widehat{\Sigma} - \Sigma\|_1$ and $\|\widehat{\Sigma} - \Sigma\|_2$ for our robust estimators (Robust B and Robust T), our proposed estimators (Proposed B and Proposed T) and the naive sample covariance estimator (Sample) are summarized in this table. The averages of \widehat{k}_1 and \widehat{k}_2 for the proposed robust/non-robust methods, the averages of $\widehat{\tau}$ for the proposed robust methods are also reported.

$(n, p, q, \rho_1, \rho_2)$	Method	$\ \widehat{\Sigma} - \Sigma\ _F$	$\ \widehat{\Sigma} - \Sigma\ _1$	$\ \widehat{\Sigma} - \Sigma\ _2$	\widehat{k}_1	\widehat{k}_2	$\widehat{\tau}$
(50, 20, 30, 0.1, 0.1)	Sample	245.38	590.03	209.47			
	Proposed B	12.64	3.02	1.97	1.24	1.13	
	Proposed T	11.79	1.66	1.32	1.10	0.86	
	Robust B	9.02	1.70	1.03	1.38	1.29	7.38
	Robust T	8.80	1.21	0.88	1.18	1.00	7.52
(50, 20, 30, 0.5, 0.5)	Sample	245.70	574.99	209.81			
	Proposed B	28.28	21.62	11.00	2.91	2.76	
	Proposed T	25.67	15.61	8.60	2.80	2.80	
	Robust B	16.70	8.05	4.49	3.24	3.24	6.17
	Robust T	16.27	7.15	4.30	3.67	3.62	5.87
(50, 20, 30, 0.8, 0.8)	Sample	249.51	511.77	212.37			
	Proposed B	103.69	177.59	76.45	11.63	11.17	
	Proposed T	91.97	148.16	66.02	11.35	11.16	
	Robust B	50.17	48.50	28.90	11.75	11.81	2.39
	Robust T	48.35	46.89	29.60	11.92	12.04	2.60

6 Real Data Application

6.1 EEG data analysis

We apply our method on an electroencephalography data, which can be downloaded at <https://archive.ics.uci.edu/ml/datasets/EEG+Database>. This dataset was collected by the Neurodynamics Laboratory as a part of a large study to examine EEG correlates of genetic predisposition to alcoholism. It contains measurements from 64 electrodes placed on subjects' scalps which were sampled at 256 Hz (3.9-msec epoch) for 1 second. Each subject was exposed to three stimuli: a single stimulus, two matched stimuli, two unmatched stimuli. In this dataset, there are 77 alcoholic individuals and 45 controls with 120 trials per subject. Detailed information can be found in [Zhang et al. \(1995\)](#). The same data set was analyzed in [Zhou and Li \(2014\)](#), where they used the average of all trials under single-stimulus condition and obtained reproducible signals with high signal-to-noise ratio. This results in covariates \mathbf{X}_i with dimensions 64×256 , where the first dimension denotes different locations of the electrodes, and second dimension denotes different time points.

In order to quantify the effect of drinking on (dynamic) connectivity in the EEG brain signals, we apply the proposed methods to estimate the covariance matrices of the alcoholic and control groups separately. For 77 alcoholic individuals, the resampling scheme with random split $N = 10$ picks $\widehat{k}_{1,A}^{\mathcal{B}} = 23$ and $\widehat{k}_{2,A}^{\mathcal{B}} = 130$ for proposed banded estimator and selects $\widehat{k}_{1,A}^{\mathcal{J}} = 61$ and $\widehat{k}_{2,A}^{\mathcal{J}} = 49$ for the proposed tapering estimator. The proposed banded and tapering estimates of the covariance $\widehat{\Sigma}_A^{\mathcal{B}}(\widehat{k}_{1,A}^{\mathcal{B}}, \widehat{k}_{2,A}^{\mathcal{B}}), \widehat{\Sigma}_A^{\mathcal{J}}(\widehat{k}_{1,A}^{\mathcal{J}}, \widehat{k}_{2,A}^{\mathcal{J}}) \in \mathbb{R}^{16384 \times 16384}$ are plotted in Figure 1(c) and Figure 2(c). We have also plotted the scaled version of $\widehat{\Sigma}_{1,A}^{\mathcal{B}}(\widehat{k}_{1,A}^{\mathcal{B}}), \widehat{\Sigma}_{1,A}^{\mathcal{J}}(\widehat{k}_{1,A}^{\mathcal{J}}) \in \mathbb{R}^{64 \times 64}$ and $\widehat{\Sigma}_{2,A}^{\mathcal{B}}(\widehat{k}_{2,A}^{\mathcal{B}}), \widehat{\Sigma}_{2,A}^{\mathcal{J}}(\widehat{k}_{1,A}^{\mathcal{J}}) \in \mathbb{R}^{256 \times 256}$ in Figures 1(a), 2(a), 1(b) and 2(b), where the maximum element of each $\widehat{\Sigma}_{1,A}^{\mathcal{B}}(\widehat{k}_{1,A}^{\mathcal{B}}), \widehat{\Sigma}_{1,A}^{\mathcal{J}}(\widehat{k}_{1,A}^{\mathcal{J}})$ and $\widehat{\Sigma}_{2,A}^{\mathcal{B}}(\widehat{k}_{2,A}^{\mathcal{B}}), \widehat{\Sigma}_{2,A}^{\mathcal{J}}(\widehat{k}_{1,A}^{\mathcal{J}})$ is scaled to be 1.

We then apply the proposed procedures to the 45 control individuals. The resampling scheme with random split $N = 10$ picks $\widehat{k}_{1,C}^{\mathcal{B}} = 36$ and $\widehat{k}_{2,C}^{\mathcal{B}} = 55$ for the proposed banded estimator and selects $\widehat{k}_{1,C}^{\mathcal{J}} = 51$ and $\widehat{k}_{2,C}^{\mathcal{J}} = 39$ for the proposed

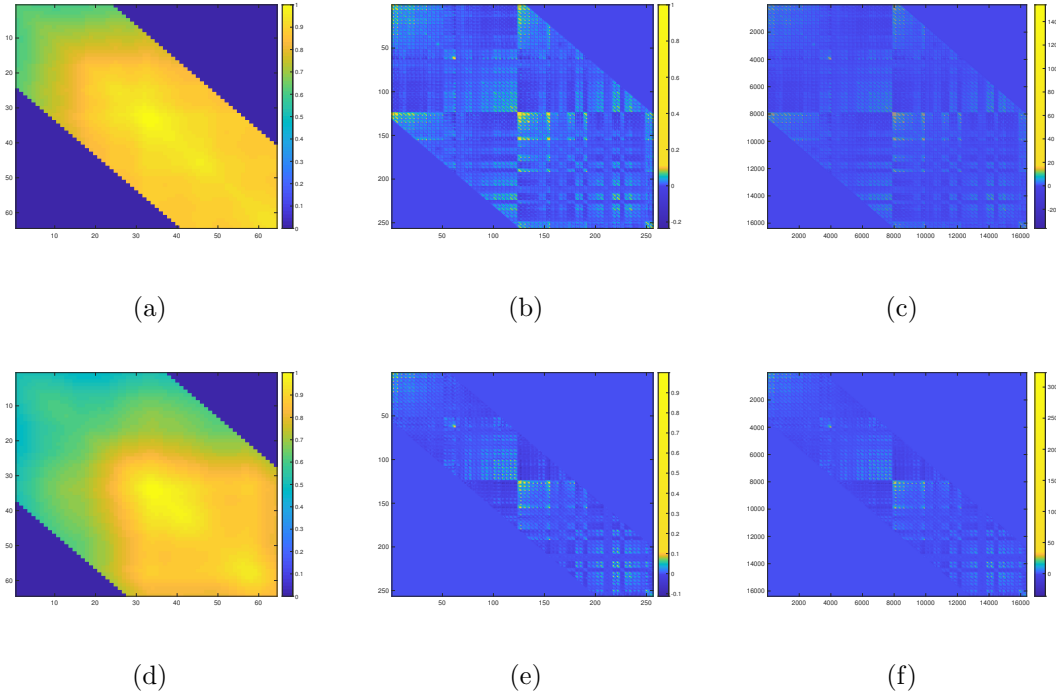


Figure 1: EEG data analysis: Plots for the estimated covariance matrices with proposed banded estimator: Panel (a) plots the scaled version of $\widehat{\Sigma}_{1,A}^{\mathcal{B}}(\widehat{k}_{1,A}^{\mathcal{B}})$, Panel (b) plots the scaled version of $\widehat{\Sigma}_{2,A}^{\mathcal{B}}(\widehat{k}_{2,A}^{\mathcal{B}})$ and Panel (c) plots the $\widehat{\Sigma}_A^{\mathcal{B}}(\widehat{k}_{1,A}^{\mathcal{B}}, \widehat{k}_{2,A}^{\mathcal{B}})$ for the alcoholic group. Panel (d) plots the scaled version of $\widehat{\Sigma}_{1,C}^{\mathcal{B}}(\widehat{k}_{1,C}^{\mathcal{B}})$, Panel (e) plots the scaled version of $\widehat{\Sigma}_{2,C}^{\mathcal{B}}(\widehat{k}_{2,C}^{\mathcal{B}})$ and Panel (f) plots the $\widehat{\Sigma}_C^{\mathcal{B}}(\widehat{k}_{1,C}^{\mathcal{B}}, \widehat{k}_{2,C}^{\mathcal{B}})$ for the control group.

tapering estimator. The estimated $\widehat{\Sigma}_{1,C}^{\mathcal{B}}$, $\widehat{\Sigma}_{2,C}^{\mathcal{B}}$, $\widehat{\Sigma}_C^{\mathcal{B}}$ and $\widehat{\Sigma}_{1,C}^{\mathcal{J}}$, $\widehat{\Sigma}_{2,C}^{\mathcal{J}}$, $\widehat{\Sigma}_C^{\mathcal{J}}$ are plotted in Figure 1(d)(e)(f) and Figure 2(d)(e)(f) respectively.

The estimated covariance matrices $\widehat{\Sigma}_{1,A}^{\mathcal{B}}$, $\widehat{\Sigma}_{1,C}^{\mathcal{B}}$ or $\widehat{\Sigma}_{1,A}^{\mathcal{J}}$, $\widehat{\Sigma}_{1,C}^{\mathcal{J}}$ reflect the strength of the functional connectivity between different regions of the brain. We can see an increased functional connectivity for the alcoholic individuals compared to controls, which coincides with the findings in the literature (Beck et al., 2012; Correias et al., 2016). The estimated covariance matrices $\widehat{\Sigma}_{2,A}^{\mathcal{B}}$, $\widehat{\Sigma}_{2,C}^{\mathcal{B}}$ or $\widehat{\Sigma}_{2,A}^{\mathcal{J}}$, $\widehat{\Sigma}_{2,C}^{\mathcal{J}}$ reflect the correlation in the temporal dimension. Clearly a bandable covariance structure fits the temporal direction variation well. The estimates for both groups show a clear periodic pattern.

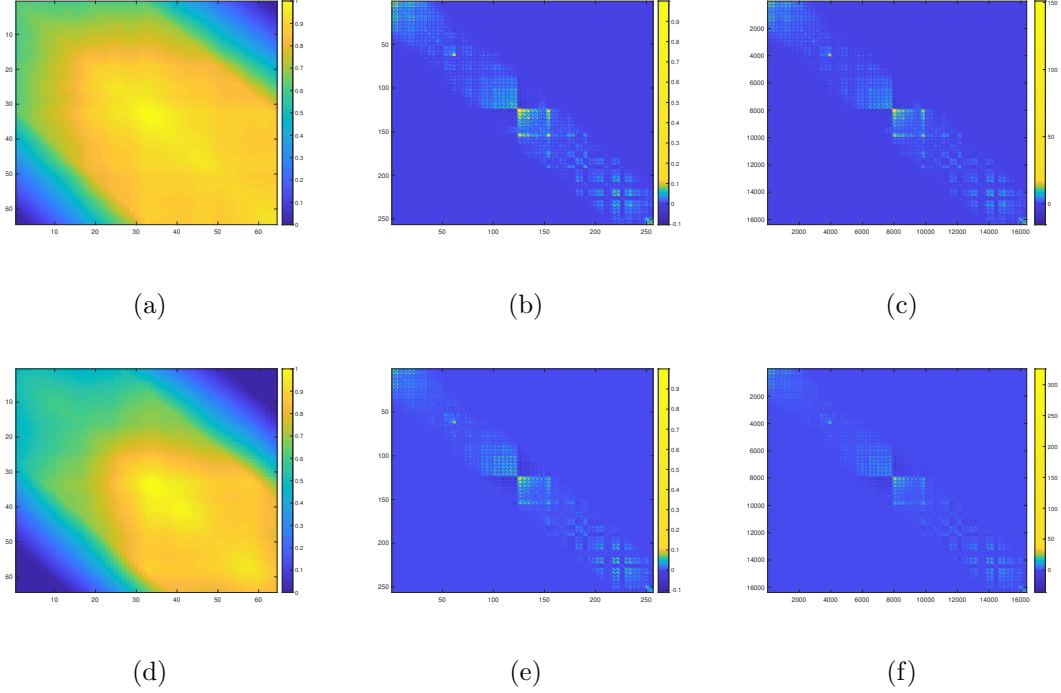


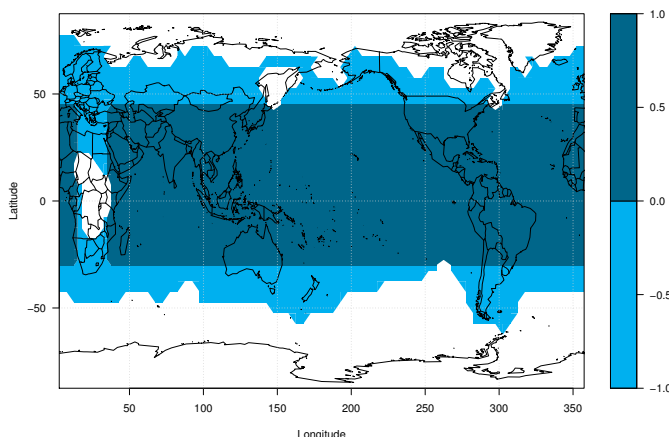
Figure 2: EEG data analysis: Plots for the estimated covariance matrices with proposed tapering estimator: Panel (a) plots the scaled version of $\widehat{\Sigma}_{1,A}^{\mathcal{J}}(\widehat{k}_{1,A}^{\mathcal{J}})$, Panel (b) plots the scaled version of $\widehat{\Sigma}_{2,A}^{\mathcal{J}}(\widehat{k}_{2,A}^{\mathcal{J}})$ and Panel (c) plots the $\widehat{\Sigma}_A^{\mathcal{J}}(\widehat{k}_{1,A}^{\mathcal{J}}, \widehat{k}_{2,A}^{\mathcal{J}})$ for the alcoholic group. Panel (d) plots the scaled version of $\widehat{\Sigma}_{1,C}^{\mathcal{J}}(\widehat{k}_{1,C}^{\mathcal{J}})$, Panel (e) plots the scaled version of $\widehat{\Sigma}_{2,C}^{\mathcal{J}}(\widehat{k}_{2,C}^{\mathcal{J}})$ and Panel (f) plots the $\widehat{\Sigma}_C^{\mathcal{J}}(\widehat{k}_{1,C}^{\mathcal{J}}, \widehat{k}_{2,C}^{\mathcal{J}})$ for the control group.

6.2 Gridded Temperature Anomaly data analysis

Next we analyze a gridded temperature anomalies dataset collected by the U.S. National Oceanic and Atmospheric Administration (NOAA) (Shen, 2017; Gu and Shen, 2020). This dataset contains the monthly air and marine temperature measurements from Jan 1880 to 2017 with a $5^\circ \times 5^\circ$ latitude-longitude resolution. It can be downloaded at <ftp://ftp.ncdc.noaa.gov/pub/data/noaaglobaltemp/operational>.

In our study, we focus on the temperature anomalies (the difference between an observed temperature and the baseline/normal value) in the past 20 years over the region marked in deep blue as shown in Figure 3 to avoid the missing values and to make sure the resulting data are in a matrix form (with two dimensions representing longitude and latitude). We pre-processed the data to remove the mean trend and the dependence over the time. This is implemented by (i) first fitting a separate linear model for each spatial coordinate over the time and then removing the estimated time trend; and (ii) “thinning” the sequence of monthly measurements by taking a monthly record from a window of every 5 months. In Figure S1 (Supplementary File), we use $5^\circ \times 5^\circ$ box centered at $57.5^\circ W$ longitude and $7.5^\circ S$ latitude as an example to show the effect of pre-processing. In (a) and (b), we show the data before and after the detrending; and in (c), we plot the estimated auto-correlation function for the thinned sequence. It can be seen that both detrending and thinning work quite well for that region. Similar results were also obtained for other spatial regions in our dataset.

After preprocessing, we obtain a dataset of 15 (latitude) \times 68 (longitude) matrix with a sample size of $n = 48$. We then apply our proposed robust banded and tapering covariance estimation methods. The threshold parameter τ for robust estimation is chosen by the method introduced in Section 4 with $\mathcal{P} = \{100, 99.995, 99.99, 99.97, 99.95, 99.9\}$. The resampling scheme chooses $\widehat{k}_1^{\mathcal{R},\mathcal{B}} = 3$, $\widehat{k}_2^{\mathcal{R},\mathcal{B}} = 12$ and $\widehat{\tau}^{\mathcal{R},\mathcal{B}} = |x|_{99.97} = 5.2761$ for the proposed robust banded estimator and picks $\widehat{k}_1^{\mathcal{R},\mathcal{T}} = 6$, $\widehat{k}_2^{\mathcal{R},\mathcal{T}} = 12$ and $\widehat{\tau}^{\mathcal{R},\mathcal{T}} = |x|_{99.995} = 6.3146$ for the proposed robust tapering estimator with random split for $N = 10$ times. The selected threshold parameter values suggest that there



(a)

Figure 3: Temperature data analysis: The whole blue region in the plot shows all non-missing spatial coordinates in [Gu and Shen \(2020\)](#)'s dataset. The deep blue region shows the spatial coordinates we extract from all non-missing coordinates to form our matrix type dataset.

are a small proportion of outliers in the data, which agrees with the boxplots in Figure S1(d) in the Supplementary File.

We plot the estimated covariance matrices in Figure 4. For (a) and (d), we have the covariance matrices along the latitude direction obtained by banding and tapering (denoted by $\widehat{\Sigma}_1^{\mathcal{R},\mathcal{B}}(\widehat{k}_1^{\mathcal{R},\mathcal{B}}), \widehat{\Sigma}_1^{\mathcal{R},\mathcal{T}}(\widehat{k}_1^{\mathcal{R},\mathcal{T}}) \in \mathbb{R}^{15 \times 15}$); longitude direction (denoted by $\widehat{\Sigma}_2^{\mathcal{R},\mathcal{B}}(\widehat{k}_2^{\mathcal{R},\mathcal{B}}), \widehat{\Sigma}_2^{\mathcal{R},\mathcal{T}}(\widehat{k}_2^{\mathcal{R},\mathcal{T}}) \in \mathbb{R}^{68 \times 68}$) for (b) and (e). All these matrices are scaled such that the maximum entry is 1. The entire covariance ($\widehat{\Sigma}^{\mathcal{R},\mathcal{B}}(\widehat{k}_1^{\mathcal{R},\mathcal{B}}, \widehat{k}_2^{\mathcal{R},\mathcal{B}}), \widehat{\Sigma}^{\mathcal{R},\mathcal{T}}(\widehat{k}_1^{\mathcal{R},\mathcal{T}}, \widehat{k}_2^{\mathcal{R},\mathcal{T}}) \in \mathbb{R}^{1020 \times 1020}$) are plotted in Figure 4 (c) and (f). In the plot, both tapering and banded methods give similar results. A bandable structure clearly fits the data well since one would expect that the association between temperatures at two distant geographic areas is very weak. For the longitude direction, there is a cluster of areas around $40^\circ N$ that has a strong correlation (lower-right corner in (a) and (d)). For the latitude direction, there are two clusters of areas with strong correlation around $50^\circ E$ and $83^\circ W$. Those coordinates correspond to the Caspian Sea and Great Lakes (USA).

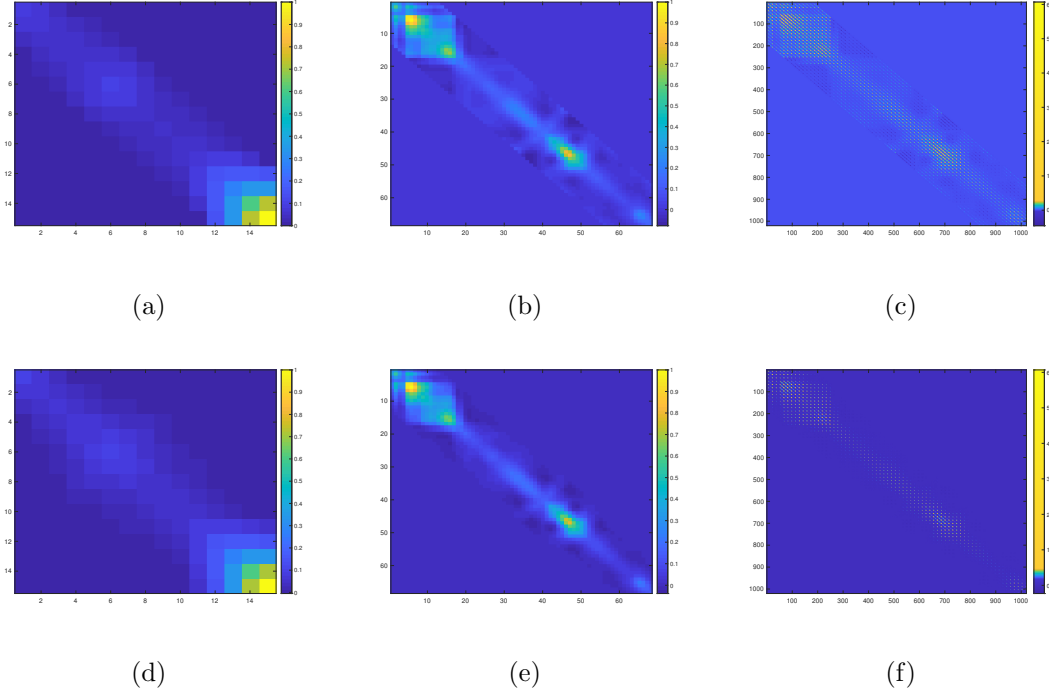


Figure 4: Temperature data analysis: Plots for the estimated covariance matrices with proposed banded and tapering estimators: Panel (a) plots the scaled version of $\widehat{\Sigma}_1^{\mathcal{R},\mathcal{B}}(\widehat{k}_1^{\mathcal{R},\mathcal{B}})$, Panel (b) plots the scaled version of $\widehat{\Sigma}_2^{\mathcal{R},\mathcal{B}}(\widehat{k}_2^{\mathcal{R},\mathcal{B}})$ and Panel (c) plots the $\widehat{\Sigma}^{\mathcal{R},\mathcal{B}}(\widehat{k}_1^{\mathcal{R},\mathcal{B}}, \widehat{k}_2^{\mathcal{R},\mathcal{B}})$. Panel (d) plots the scaled version of $\widehat{\Sigma}_1^{\mathcal{R},\mathcal{T}}(\widehat{k}_1^{\mathcal{R},\mathcal{T}})$, Panel (e) plots the scaled version of $\widehat{\Sigma}_2^{\mathcal{R},\mathcal{T}}(\widehat{k}_2^{\mathcal{R},\mathcal{T}})$ and Panel (f) plots the $\widehat{\Sigma}^{\mathcal{R},\mathcal{T}}(\widehat{k}_1^{\mathcal{R},\mathcal{T}}, \widehat{k}_2^{\mathcal{R},\mathcal{T}})$.

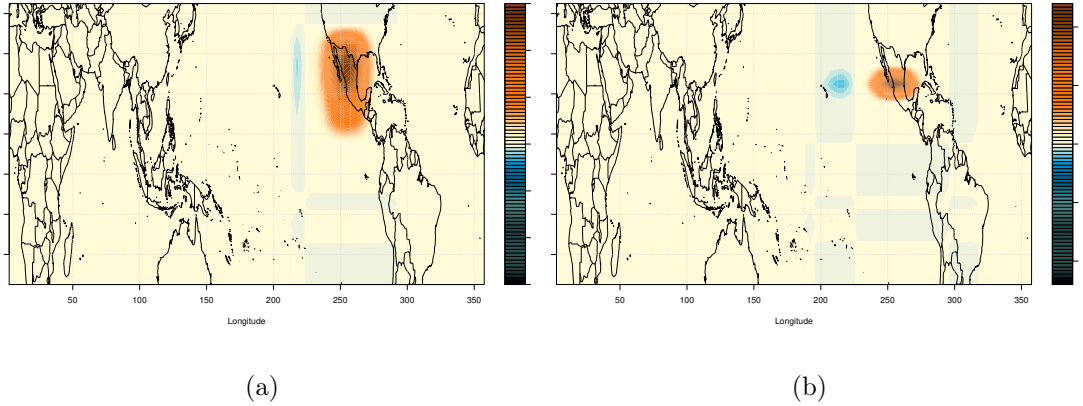


Figure 5: Temperature data analysis: Panel (a) plots the proposed banded covariance estimation of each lat-lon box with the lat-lon box centered at $107.5^{\circ}W$ longitude and $22.5^{\circ}N$ latitude. Panel (b) plots the proposed tapering covariance estimation of each lat-lon box with the lat-lon box centered at $107.5^{\circ}W$ longitude and $22.5^{\circ}N$ latitude.

To further illustrate the use of our estimated covariance for the matrix-valued data, we focus on the $5^{\circ} \times 5^{\circ}$ box centered at $107.5^{\circ}W$ longitude and $22.5^{\circ}N$ latitude (target region: west coast side of Mexico), and study its covariance with the temperature at other regions. The results obtained by banding and tapering are summarized in Figure 5. From the plot, there are two regions that have a strong correlation with the target region. The first one marked in red is essentially the target region itself, which suggests a strong self-correlation in the neighborhood areas around the target region. The second marked in blue corresponds to ocean area (northeastern direction) near Hawaiian islands and they have a strong negative correlation, which may be related to the recent studies on LandOcean Surface Temperature ratio ([Lambert et al., 2011](#)).

7 Discussion

In this paper, we propose banded and tapering covariance estimators for matrix-valued data under a separability condition. We adopt an efficient computational

algorithm and derive the convergence rates of our covariance estimates under various scenarios. To deal with heavy-tailed data, we further propose robust banded and tapering covariance estimators, and show their theoretical advantages. We demonstrate our methods using numerical studies and real data applications from an electroencephalography study and a gridded temperature anomalies study.

There are a number of important directions for further investigation. First, the optimality of the convergence rate in Theorem 3.1 is unclear. It would be interesting to study the optimal convergence rate of our estimators. Second, our method is applicable only to the matrix-valued data. In many applications, the data can have more complex structures, such as tensor. Extension of the current approach to tensor-valued data is highly non-trivial in both computation and theory. Therefore, we leave it for future research.

References

- Batselier, K. and N. Wong (2017). A constructive arbitrary-degree kronecker product decomposition of tensors. *Numerical Linear Algebra with Applications* 24(5), e2097.
- Beck, A., T. Wüstenberg, A. Genauck, J. Wrase, F. Schlagenhaut, M. N. Smolka, K. Mann, and A. Heinz (2012). Effect of brain structure, brain function, and brain connectivity on relapse in alcohol-dependent patients. *Archives of General Psychiatry* 69(8), 842–852.
- Bickel, P. J. and E. Levina (2008a). Covariance regularization by thresholding. *The Annals of Statistics* 36(6), 2577–2604.
- Bickel, P. J. and E. Levina (2008b). Regularized estimation of large covariance matrices. *The Annals of Statistics* 36(1), 199–227.
- Cai, T. and W. Liu (2011). Adaptive thresholding for sparse covariance matrix estimation. *Journal of the American Statistical Association* 106(494), 672–684.

- Cai, T. T., C.-H. Zhang, and H. H. Zhou (2010). Optimal rates of convergence for covariance matrix estimation. *The Annals of Statistics* 38(4), 2118–2144.
- Castillo-Barnes, D., I. Peis, F. J. Martínez-Murcia, F. Segovia, I. A. Illán, J. M. Górriz, J. Ramírez, and D. Salas-Gonzalez (2017). A heavy tailed expectation maximization hidden markov random field model with applications to segmentation of MRI. *Frontiers in Neuroinformatics* 11, 66.
- Cont, R. (2001). Empirical properties of asset returns: stylized facts and statistical issues.
- Correas, A., P. Cuesta, E. López-Caneda, S. R. Holguín, L. García-Moreno, J. Pineda-Pardo, F. Cadaveira, and F. Maestú (2016). Functional and structural brain connectivity of young binge drinkers: a follow-up study. *Scientific Reports* 6, 31293.
- Dawid, A. P. (1981). Some matrix-variate distribution theory: notational considerations and a Bayesian application. *Biometrika* 68(1), 265–274.
- De Munck, J. C., H. M. Huizenga, L. J. Waldorp, and R. Heethaar (2002). Estimating stationary dipoles from meg/eeg data contaminated with spatially and temporally correlated background noise. *IEEE Transactions on Signal Processing* 50(7), 1565–1572.
- Dutilleul, P. (1999). The mle algorithm for the matrix normal distribution. *Journal of Statistical Computation and Simulation* 64(2), 105–123.
- El Karoui, N. (2008). Operator norm consistent estimation of large-dimensional sparse covariance matrices. *The Annals of Statistics* 36(6), 2717–2756.
- Fan, J., W. Wang, and Z. Zhu (2016). A shrinkage principle for heavy-tailed data: High-dimensional robust low-rank matrix recovery. *arXiv preprint arXiv:1603.08315*.

- Friston, K. J., P. Jezzard, and R. Turner (1994). Analysis of functional MRI time-series. *Human Brain Mapping* 1(2), 153–171.
- Fuentes, M. (2006). Testing for separability of spatial–temporal covariance functions. *Journal of Statistical Planning and Inference* 136(2), 447–466.
- Furrer, R. and T. Bengtsson (2007). Estimation of high-dimensional prior and posterior covariance matrices in Kalman filter variants. *Journal of Multivariate Analysis* 98(2), 227–255.
- Galecki, A. T. (1994). General class of covariance structures for two or more repeated factors in longitudinal data analysis. *Communications in Statistics-Theory and Methods* 23(11), 3105–3119.
- Golub, G. and C. VanLoan (1996). Matrix computations.
- Gu, M. and W. Shen (2020). Generalized probabilistic principal component analysis of correlated data. *Journal of Machine Learning Research* 21(13), 1–41.
- Hoff, P. D. (2011). Separable covariance arrays via the Tucker product, with applications to multivariate relational data. *Bayesian Analysis* 6(2), 179–196.
- Johnstone, I. M. (2001). On the distribution of the largest eigenvalue in principal components analysis. *The Annals of Statistics* 29(2), 295–327.
- Johnstone, I. M. and A. Y. Lu (2009). On consistency and sparsity for principal components analysis in high dimensions. *Journal of the American Statistical Association* 104(486), 682–693.
- Kong, D., B. An, J. Zhang, and H. Zhu (2020). L2RM: Low-rank linear regression models for high-dimensional matrix responses. *Journal of the American Statistical Association* 115(529), 403–424.
- Lambert, F. H., M. J. Webb, and M. M. Joshi (2011). The relationship between landocean surface temperature contrast and radiative forcing. *Journal of Climate* 24(13), 3239–3256.

- Liu, L., D. M. Hawkins, S. Ghosh, and S. S. Young (2003). Robust singular value decomposition analysis of microarray data. *Proceedings of the National Academy of Sciences* 100(23), 13167–13172.
- Lu, N. and D. L. Zimmerman (2005). The likelihood ratio test for a separable covariance matrix. *Statistics & Probability Letters* 73(4), 449–457.
- Mitchell, M. W., M. G. Genton, and M. L. Gumpertz (2006). A likelihood ratio test for separability of covariances. *Journal of Multivariate Analysis* 97(5), 1025–1043.
- Pitsianis, N. P. (1997). *The Kronecker product in approximation and fast transform generation*. Ph. D. thesis, Cornell University.
- Purdom, E. and S. P. Holmes (2005). Error distribution for gene expression data. *Statistical Applications in Genetics and Molecular Biology* 4(1).
- Shen, S. (2017). R programming for climate data analysis and visualization: Computing and plotting for NOAA data applications. *The first revised edition*. San Diego State University, San Diego, USA.
- Van Loan, C. F. and N. Pitsianis (1993). Approximation with kronecker products. In *Linear Algebra for Large Scale and Real-time Applications*, pp. 293–314. Springer.
- Visser, H. and J. Molenaar (1995). Trend estimation and regression analysis in climatological time series: an application of structural time series models and the kalman filter. *Journal of Climate* 8(5), 969–979.
- Wachter, K. W. et al. (1978). The strong limits of random matrix spectra for sample matrices of independent elements. *The Annals of Probability* 6(1), 1–18.
- Wang, X. and H. Zhu (2017). Generalized scalar-on-image regression models via total variation. *Journal of the American Statistical Association* 112(519), 1156–1168.
- Werner, K., M. Jansson, and P. Stoica (2008). On estimation of covariance matrices with kronecker product structure. *IEEE Transactions on Signal Processing* 56(2), 478–491.

Wu, W. B. and M. Pourahmadi (2009). Banding sample autocovariance matrices of stationary processes. *Statistica Sinica* 19(4), 1755–1768.

Zhang, X. L., H. Begleiter, B. Porjesz, W. Wang, and A. Litke (1995). Event related potentials during object recognition tasks. *Brain Research Bulletin* 38(6), 531–538.

Zhou, H. and L. Li (2014). Regularized matrix regression. *Journal of the Royal Statistical Society: Series B (Statistical Methodology)* 76(2), 463–483.